NATIONAL ADVISORY COMMITTEE FOR AERONAUTICS

TECHNICAL NOTE 2847

SECTION CHARACTERISTICS OF A 10.5-PERCENT-THICK AIRFOIL WITH AREA SUCTION AS AFFECTED BY CHORDWISE DISTRIBUTION OF PERMEABILITY

By Robert E. Dannenberg and James A. Weiberg

Ames Aeronautical Laboratory
Moffett Field, Calif.

NACA

Washington
December 1952

NATIONAL ADVISORY COMMITTEE FOR AERONAUTICS

TECHNICAL NOTE 2847

SECTION CHARACTERISTICS OF A 10.5-PERCENT-THICK AIRFOIL WITH AREA SUCTION AS AFFECTED BY CHORDWISE DISTRIBUTION OF PERMEABILITY

By Robert E. Dannenberg and James A. Weiberg

SUMMARY

An investigation has been made at low speed of the two-dimensional aerodynamic characteristics of a 10.51-percent-thick symmetrical airfoil with area suction near the leading edge. The chordwise extent and distribution of porosity were adjusted for the purpose of obtaining a low quantity of suction-air flow for the maximum possible lift.

The maximum lift coefficient of the basic airfoil was 1.3. A lift coefficient of 1.71 was obtained with a section flow coefficient of 0.0008, and a maximum lift coefficient of 1.78 was obtained with a section flow coefficient of 0.0014.

It was found that for a given lift coefficient a very low power would be required for suction, provided a suitable permeability and arrangement of porous material were employed. The flow resistance characteristics of some porous materials that might be used to provide such a surface are given.

INTRODUCTION

The attainment of high lift and good stalling characteristics on moderately thick (9 to 12 percent) wing sections involves the control of the separation of the air flow in the boundary layer near the leading edge. The use of devices such as leading-edge flaps and slats has been directed toward this end (reference 1). Control of the boundary layer has also been attempted by means of suction through a slot or through a porous area near the leading edge of the airfoil (references 2 to 5). Theoretical considerations (reference 4) have shown that the suction-air quantity required to produce a given lift coefficient can be less for suction over a porous area than through a slot. With area suction the problem is one of attaining the desired lift with minimum power. The primary variables

involved are the extent of porous area, the suction velocity required, and the surface and flow-resistance characteristics of the porous area. For a practical application, other considerations such as strength and serviceability (clogging, etc.) must be considered.

To investigate means of reducing the suction-flow quantity and power requirements of area suction for increasing maximum lift, a symmetrical airfoil with a maximum thickness of 10.51-percent chord at 35-percent chord was tested in the Ames 7- by 10-foot wind tunnel. The effects of variations of chordwise distributions of permeability were investigated from considerations of both the section lift and the suction-power requirements. The tests included measurements of the surface pressure distributions, momentum drag, and boundary-layer characteristics.

Measurements were also made of the flow-resistance characteristics of various types of porous media suitable for use as surface materials in area suction tests.

NOTATION

The symbols used in this report are defined as follows:

c wing chord, feet

c_{d_o} section profile-drag coefficient $\left(\frac{D}{q_o c}\right)$

c_{d_T} section total-drag coefficient $(c_{d_o} + c_w)$

c_l section lift coefficient $\left(\frac{L}{q_o c}\right)$

c_m section pitching-moment coefficient referred to the quarter chord $\left(\frac{M}{q_o c^2}\right)$

c_Q section flow coefficient through the outer surface of the porous area $\left(\frac{\int v ds}{c\, U_o}\right)$

(The limits of integration are the foremost and rearmost chordwise points of area suction.)

c_w section power drag coefficient

$$\left\{ \frac{1}{c q_o U_o} \left(\frac{\gamma}{\gamma - 1}\right) Q_1 p_1 \left[\left(\frac{p_o}{p_1}\right)^{\frac{\gamma-1}{\gamma}} - 1 \right] \right\}$$

D	drag per unit span, pounds
H	boundary-layer shape parameter $\left(\frac{\delta^*}{\theta}\right)$
Δh	total-pressure loss, inches of water
L	lift per unit span, pounds
M	pitching moment per unit span, pound-feet
P	pressure coefficient $\left(\frac{p-p_o}{q_o}\right)$
p	static pressure, pounds per square foot
Q	volume rate of flow per unit span, cubic feet per second
q_o	free-stream dynamic pressure $\left(\frac{1}{2}\rho_o U_o^2\right)$, pounds per square foot
s	distance along airfoil surface, feet
U	local velocity outside boundary layer, feet per second
U_o	free-stream velocity, feet per second
u	local velocity within boundary layer, feet per second
v	suction-air velocity, normal to outer surface of the airfoil, feet per second
v_{min}	suction-air velocity at the point of minimum external pressure, feet per second
x	distance from airfoil leading edge measured parallel to chord line, feet
y	distance from airfoil measured normal to surface, feet
α	angle of attack, degrees
γ	ratio of specific heats for air, taken as 1.4
δ	total boundary-layer thickness, feet
δ^*	boundary-layer displacement thickness $\left[\int_o^\delta \left(1-\frac{u}{U}\right)dy\right]$, feet

θ boundary-layer momentum thickness $\left[\int_0^{\delta} \frac{u}{U}\left(1-\frac{u}{U}\right) dy\right]$, feet

τ index of resistivity, defined as the total pressure difference in inches of water required to induce a suction-air velocity normal to the surface of 1 foot per second through a porous material of a given thickness

φ exponent value used in the equation $\Delta h = \tau v^{\varphi}$ to define the flow-resistance characteristics of a given porous material

ρ mass density of air, slugs per cubic foot

Subscripts

e local external point

o free-stream conditions

1 conditions in suction duct

min minimum

u uncorrected

SELECTION OF POROUS MATERIAL

In the experiments contemplated for the wing with area suction, it was proposed to study the effect of a range of suction-air velocities from about 0.2 to 10 feet per second. The pressure differences across the porous media necessary to induce these velocities were to be of the order of 1 to 100 inches of water. A number of different types of porous materials were investigated that would satisfy the various requisite pressure difference and velocity characteristics.

The flow resistance characteristics of the various porous materials tested are tabulated in table I. A detailed description of the materials is given in the references noted in the table. As three general types of porous media were tested, granular, fibrous, and perforated, a problem arose in selecting the form for presenting the results of the porous specimen tests in a usable manner. For sintered metals and possibly ceramics, the results could have been presented in terms of a permeability coefficient that satisfies Darcy's law for flow through granular media (reference 6). A discussion of the application of Darcy's law to flow

through fibrous media is given in reference 7. For the purpose of the present investigation, the results have been presented in equation form relating the velocity to the head loss by

$$\Delta h = \tau v^{\varphi}$$

The values of τ and φ are tabulated in table I for materials of various thicknesses.

Examination of the characteristics of the porous materials tested indicated that three classes of materials were available that satisfied the requirements of the experiments contemplated: filter paper, felt, and sintered metals. For the purpose of the investigation of this report, filter paper was selected as the material to be used.

MODEL AND APPARATUS

Model

The 4.5-foot-chord, two-dimensional model used for this investigation is shown in figure 1. Coordinates of the 10.51-percent-thick, symmetrical airfoil section and a sketch of the profile are given in table II. For comparison, the profile of a symmetrical NACA 4-digit 00-series airfoil of equal maximum thickness is also shown in the sketch. Flush orifices in the outer surface of the model permitted measurement of the pressure distribution.

Tunnel-wall boundary-layer interference effects necessitated an end plate and slat arrangement, as shown in figure 1. The span between the end plates was 5 feet. The slats were located between the end plates and the tunnel walls. Pertinent dimensions of the end plates and slats are given in table III.

For the tests of the plain wing, a solid wood nose section was used. For the suction tests, a porous nose section was used. The model contained an internal plenum chamber and ducting for the porous nose sections. A typical section through the model is shown in figure 2. Static-pressure tubes were used to measure the internal pressures. The cross-section area of the internal plenum chamber and ducting was large enough to reduce the dynamic head of the induced air to negligible values and to insure uniform internal pressures across the span of the model.

The permeable material used for the porous surface of the model was a commercial grade of filter paper (materials 1 and 2 of table I). The filter paper was supported over a 16-mesh (0.023 diam. wire) wire cloth, backed by a second rigid 3-mesh (0.063 diam. wire) wire cloth. The wire cloths were fastened to ribs spaced at 6-inch intervals, as shown in figure 2. The filter paper was fastened to the surface with a water

soluble glue, and extended from 6-percent chord on the upper surface to 1-percent chord on the lower surface.

Apparatus

The suction pressure required to induce flow through the porous material was provided by a variable-speed compressor located outside the wind tunnel. Air was drawn through the porous nose into the hollow spar in the wing and then through the ducting system to the compressor.

Boundary-layer measurements were made with a small pressure rake attached to the surface of the model. Two rakes of different heights were used, depending on the boundary-layer thickness. A larger survey rake connected to an integrating manometer was used to measure wake pressures for the calculation of wake drag.

TEST METHODS

Air flow through the porous area of the airfoil was induced by maintaining a pressure inside the model that was less than the value of the minimum external pressure as illustrated in figure 3. The suction-air velocity at a given chordwise station was calculated from the measured pressure difference across the porous material and the flow resistance characteristics of the porous material given in figure 4. For a uniform porous material of constant thickness, the pressure differences across the material induced flow velocities normal to the surface that were a minimum[1] at the point of minimum external pressure and increased in magnitude in the chordwise direction, as indicated in figure 3. The method of obtaining data was (1) to maintain various constant values of suction-flow velocity v_{min} at the position of minimum pressure on the wing as an angle of attack was varied, or (2) to maintain various constant angles of attack as the v_{min} was varied. The largest value of this suction velocity at the position of minimum pressure was limited by the blower system. The smallest value was limited to the condition of no outflow through the porous area.

Measurements of pressure distributions and boundary layers at various angles of attack were made at a test Mach number of 0.14 and a Reynolds number of 4,370,000 based on the wing chord. Wake drag data were obtained for a Reynolds number of 5,030,000. The lift and pitching-moment characteristics were calculated from graphical integration of the chordwise distributions of pressure. The section flow coefficients were calculated from integration of the suction velocity along the porous surface. The wake pressures used in calculation of the profile drag were measured by a

[1]Referred to herein as v_{min}.

survey rake that was located one-half-chord length behind the wing trailing edge. The total profile drag coefficient was taken to be equal to the power drag coefficient c_w plus the profile coefficient c_{d_o}.

Tunnel-wall corrections, as described in reference 8, have not been applied to the data. The correction in degrees usually added to the angle of attack for correcting the data to free-air conditions would be 0.384 times the section lift coefficient.

The flow-resistance characteristics of the various porous materials were obtained by means of the apparatus shown in figure 5. The test setup consisted of a 5-inch-diameter pipe in which the specimen under test was clamped between flanges of the pipe. The air flow through the material was induced by a variable-speed compressor. The rate of air flow was measured by means of a standard A.S.M.E. orifice. The pressure loss across the material was measured by means of pipe taps. As some of the materials tested were nonrigid, it was necessary to back the materials with a 16-mesh (0.023 diam. wire) wire cloth as shown in figure 5(b). The pressure loss across the wire cloth was negligible through the range of air flow tested.

RESULTS AND DISCUSSION

Plain Wing

Evaluation of the effects of area suction as a means of boundary-layer control can be made by comparison of the results for the plain wing with those for the wing with area suction. The question arises, however, as to the type of plain wing surface condition that should be used as a basis for the comparison. With the permeable nose sections, the surface would be considered as a "rough surface" because of the filter paper covering. For this reason, tests were made of the plain wing with both smooth and rough surface conditions. The rough surface condition consisted of a single thickness of filter paper glued to the wing in exactly the same position as used with the porous nose sections.

The lift, profile drag, and pitching-moment coefficients of the plain wing for both surface conditions are given in figure 6.

Smooth surface condition.- The data in figure 6 for the smooth surface condition show characteristics similar to those of moderately thin wing sections which stall from the leading edge (reference 9). This type of stall is characterized by abrupt changes in the lift and pitching moment when the angle of attack for maximum lift is exceeded, with little or no rounding over of the lift curve near maximum lift. The inerease in drag with lift is moderate up to the stall. The chordwise pressure distributions in figure 7 show a gradual increase in the peak negative

pressures up to the stall followed by an abrupt collapse with a redistribution of the pressures chordwise, giving the flat-type pressure distribution characteristic of separated flow. This redistribution of pressure after the stall results in a rearward shift in the center of pressure and the abrupt negative shift in pitching moment shown in figure 6.

The pressure data were plotted for given chordwise stations against angle of attack in figure 8(a) to indicate the pressure discontinuities which have been shown by reference 9 to be indicative of the presence of a localized region of laminar separation followed by transition and reattachment of the turbulent boundary layer. The discontinuities in the curves shown in figure 8(a), caused by the passage of the separation bubble over the orifice, result from the relatively constant pressure within the bubble. The discontinuities in the pressure data were first noticeable at the 2.5-percent-chord station for an angle of attack of 5.5°. The data showed that the pressure discontinuity gradually moved forward on the airfoil with increasing angle of attack and reached the 1.0-percent-chord station at maximum lift (12° angle of attack).

Rough surface condition.- The lift, profile drag, and pitching-moment coefficients of the plain wing with the rough surface condition (filter paper from 1-percent chord on the lower surface to 6-percent chord on the upper surface) are given in figure 6. These data indicate that the addition of roughness to the leading edge resulted in an increase in the profile drag and a decrease in maximum lift coefficient from 1.30 to 1.15. There was little change in the stalling and pitching-moment characteristics other than that associated with the decrease in maximum lift.

The chordwise distributions of pressure were similar to those of the wing in the smooth condition (fig. 7) except for an area near the leading edge, as indicated in figure 8(b). The discontinuities in the pressure-coefficient variation near the leading edge were noticeable for given orifice stations at lower angles of attack.

Wing With Various Chordwise Extents of Area Suction

The determination of the optimum chordwise extent of suction for maximum lift was made using the wing with the nose section porous from 0- to 5-percent chord on the upper surface with a single thickness sheet of filter paper as the permeable material (material 1 of table I and fig. 4). The effect on maximum lift of progressively closing off various portions of the porous surface with a nonporous tape is shown in figure 9 for values of the minimum suction velocity v_{min} of 1 and 5 feet per second (a v_{min}/U_o of 0.006 and 0.031, respectively). For values of v_{min} of 5 feet per second or greater, the lift coefficient attainable

remained relatively constant. The section flow coefficients are given in figure 10. Included in figure 9 is the lift curve of the plain wing for the smooth surface condition.

Figure 9 shows that reducing the chordwise extent of area suction to less than about 3-percent chord results in a decrease in maximum lift. With suction over more than 3-percent chord, the value of the maximum lift was not changed appreciably but the quantity of suction flow required was increased (fig. 10). This was true for minimum suction velocities v_{min} of 1 and 5 feet per second although the value of maximum lift and the corresponding quantity of suction flow was less for the lower suction velocity.

Thwaites, in reference 5, presents a theoretical discussion of the application of area suction for two-dimensional wing sections. A method is put forth whereby the chordwise extent of suction necessary to overcome separation can be estimated from the extrapolated pressure distributions of the wing without suction. The distance over which the suction should be applied need extend only to the chordwise station at which the adverse velocity gradient corresponding to the desired lift coefficient is no more severe than the maximum velocity gradient reached on the wing without suction prior to the stall.

Applying the method of reference 5 to the wing of the present investigation, the chordwise extent of area suction required to attain a lift coefficient of 1.8 is indicated to be approximately 3 percent. This value is in good agreement with the experimentally determined value (fig. 9). Applying the same analysis to the data of reference 3 also shows good agreement.

Wing With Area Suction From the Leading Edge to 3-Percent Chord

With the nose section porous from the leading edge to 3-percent chord (chosen on the basis of the data presented above), the effect on suction-flow quantities and power required to obtain a given lift due to changes in the distribution and flow resistance characteristics of the permeable surface material were investigated. Variations in the chordwise distribution of resistivity of the porous material were obtained with four arrangements of materials 1 and 2 of table I. The arrangements tested are designated configurations A, B, C, and D and are shown diagrammatically in figure 2. Configurations A and B have constant thickness of materials 1 and 2, respectively, over the porous area. Configurations C and D are combinations of materials 1 and 2; material 1 covers the entire porous section of the nose, while material 2 extends over part of the porous area. With this arrangement of the porous material, an abrupt discontinuity in the total resistivity occurred where material 2

terminated and resulted in a discontinuous or "stepped" distribution of suction-air velocity.

Lift and flow characteristics.- The variation of lift coefficient with angle of attack for each of the four configurations is given in figure 11 for various values of the suction velocity v_{min}. The corresponding suction pressures, flow coefficients, and power drag coefficients are shown in figure 12. The power drag coefficients were computed by the method given in the appendix. Figure 11 indicates that, with suction, the attainable maximum lift coefficient is dependent on the minimum suction-air velocity v_{min}. This is further illustrated in figures 13 and 14 which show the variations with flow coefficient and v_{min} of the maximum lift and the lift coefficient for an angle of attack near that for maximum lift. Included in the figures are the chordwise distributions of suction velocities at constant values of either flow coefficient or lift coefficient. As the minimum suction velocity v_{min} was increased, the lift coefficient, both the maximum and at constant angle of attack, increased up to a certain critical value of velocity, above which the lift coefficient attainable remained relatively constant. For configurations B and D, v_{min} was limited by the blower system because of the high resistivity of the porous material. For configuration A with a minimum suction velocity of 4 feet per second (v_{min}/U_o of 0.025) a maximum lift coefficient of 1.8 was obtained (fig. 13). It should be pointed out that it is difficult to obtain consistent data at maximum lift because of the effects small changes in the surface condition of the model and the porous leading edge have on the stall. Therefore a better comparison of the flow characteristics with the different arrangements of porous materials can be made at an angle of attack below the stall, as shown in figure 14. At 16° angle of attack, a lift coefficient of 1.71 was obtained with configurations A, B, and C with a critical minimum suction velocity of the order of 4 to 5 feet per second (a v_{min}/U_o of 0.025 to 0.031).

A comparison of the suction-velocity diagrams for configurations A and C, as shown in figure 14(b), indicates a marked difference in the section flow coefficient required to attain a lift coefficient of 1.71. Satisfactory lift characteristics were obtained for configuration C with suction velocities as low as 2 feet per second with a suction velocity at minimum external pressure v_{min} of 5 feet per second. In the case of configuration B, the section flow coefficient was less than that of configuration A for a given v_{min} but the high flow-resistance characteristics of the porous material necessitated a low plenum-chamber pressure and resulted in a high section power drag coefficient (fig. 12).

Drag and moment.- The profile drag and moment characteristics of the plain wing and the wing with suction (configuration A) are presented in figure 15. Included in this figure are total drag characteristics of the wing with suction.

The effect of suction was to reduce the profile drag over that for the wing with the rough surface condition, particularly for high lift coefficients. At low lift coefficients, roughness of the suction surface probably caused early transition. As the incidence was increased up to a lift coefficient of approximately 0.5, the profile drag decreased for the wing both in the rough surface condition and with suction. This decreasing drag with increasing lift may be explained by the fact that the transition point on the lower surface probably moved back, whereas the transition point on the upper surface remained relatively fixed.

The profile drag of the model with suction was a function of the minimum suction-air velocity v_{min} as shown in figure 15(b) for configuration A. Above a v_{min} of approximately 5 feet per second the drag was relatively constant; below this value of minimum suction velocity the drag increased with decreasing minimum suction velocity. Although the use of area suction caused relatively large decreases in the profile drag, when the section power drag (i.e., the drag equivalent of the suction power) is included, area suction is seen not to reduce the total drag except possibly in some cases for high lift coefficients.

External pressure distribution.- The chordwise distributions of the external pressure coefficients on the model with suction are shown in figure 16 for values of the minimum suction velocity of 2 and 5 feet per second. The data in this figure are for configuration A but are typical for all configurations below the angle of attack at which maximum lift occurred. In figure 17, the variation of the pressure coefficients at 10-, 40-, and 80-percent chord with angle of attack are presented for the four configurations along with similar data for the plain wing. For chordwise locations aft of 10-percent chord, the pressure coefficients at a given angle of attack were the same for the plain wing and configurations A, B, C, and D with suction.

The variations of the pressure coefficients near the leading edge with angle of attack for configurations A, B, and C are shown in figure 18. Pressure coefficients at 0- and 2-percent chord are presented for configuration A only but are typical of the other configurations. At 0.6- and 1.2-percent chord the variation of pressure coefficient with angle of attack is discontinuous, having a region of relatively constant pressure which, as mentioned previously, was shown by reference 9 to be indicative of a region of laminar separation.

Boundary-Layer Measurements

The results of surveys of the boundary layer at 10- and 95-percent chord of the wing are presented in figures 19, 20, and 21 in the form of velocity profiles and the derived boundary-layer momentum thickness θ/c and shape parameter H. Data are presented for the plain wing and the wing with 3-percent chordwise extent of suction (configuration A).

Figure 19 presents the boundary layer at 10-percent chord on the wing with suction for angles of attack of 15° and 16° for minimum suction velocities up to 8 feet per second. No measurements were made of the boundary layer at 10-percent chord on the plain wing. The boundary-layer momentum thickness for the wing with suction increases rapidly with decreasing minimum suction-air velocities below approximately 5 feet per second as would be expected from the drag and lift results.

The stall of the plain wing (smooth surface condition) was abrupt (see fig. 6). The boundary-layer shape parameter H for 95-percent chord was 2.1 at the stall (fig. 21). A value of 2.6 to 2.7 is considered to be indicative that separation of the turbulent boundary layer has occurred (references 9 and 10). On the basis of these data, it is believed that the stall without suction was not caused by separation of the turbulent boundary layer. The type of stall that limited the maximum lift of the plain wing may be classified as leading-edge stall, as defined in reference 9.

With suction, the shape parameter H attains values of the order of 2.5 to 2.7 that were dependent on the minimum suction-air velocity (fig. 21). These data indicate that the stall of the wing with suction probably resulted from turbulent separation from the trailing edge. With the small change in the shape parameter resulting from increasing the minimum suction-air velocity from 5 to 8 feet per second, it is doubtful if minimum suction-air velocities in excess of 8 feet per second would be effective in further increasing the maximum lift. Subsequent increases in the maximum lift would be dependent on a more effective means of control of the turbulent boundary layer.

Stagnation Location

Examination of the pressure-distribution data showed a change in the position of stagnation for the wing with suction compared to that for the plain wing, as shown in figure 22. The stagnation point was found by plotting the pressure data for a given orifice-measuring station against angle of attack. To compare these data with potential-flow theory, the stagnation positions were calculated for a Joukowski airfoil of the same leading-edge radius and a Joukowski airfoil whose coordinates match closely the plain wing coordinates in the nose region (L.E.R. = 0.0102c). The computed values are also shown in figure 22 compared to the plain wing. For angles of attack from 5° to 12°, suction resulted in a forward movement of the stagnation position on the wing compared to that for the plain wing. Above an angle of attack of 12°, the stagnation position with suction approached that indicated from potential flow considerations of a plain wing.

ANALYSIS OF POWER REQUIREMENTS

Previously in the discussion the effectiveness of area suction has been indicated primarily in terms of the external aerodynamic coefficients. These qualities, however, do not provide an adequate means of judging the over-all effectiveness of area suction because no account has been taken of the power required for suction.

The determination of the porous material arrangement for minimum power is governed by the suction-air-velocity distribution necessary to obtain a given lift coefficient at a prescribed free-stream velocity. The suction-air velocity and distribution of velocity and the suction pressure are related directly to the resistivity of the material used for the porous area. The suction power is a function of the chordwise extent of the porous area, the suction pressure necessary to induce the requisite flow through the porous material and the velocity of the free stream.

In order to show the effects of different flow-resistance characteristics of the porous material on the power required for suction, calculations were made of the power drag coefficients c_w of the wing of the present investigation, assuming various materials for the porous area. The results will not be dependent on the material itself but rather on the index of resistivity τ of the material. Porous materials with equal flow-resistance characteristics will exhibit equal suction-power requirements. The effects of surface roughness on the power were not considered. The calculations were made following the procedure previously discussed under the section Test Methods, assuming the porous area to extend from 0- to 3-percent chord and using an external pressure distribution equal to that of configuration A for a v_{min} of 5 feet per second. The computations are for a dynamic pressure q_0 of 30 pounds per square foot.

Results are presented for constant chordwise distribution of resistivity and for variable resistivity.

Constant Resistivity

Calculations were made assuming that the porous surface of the wing consisted of a constant thickness of uniform material for each of the porous media represented in figure 23. The computations were made for assumed section lift coefficients of 1.71 and 1.44 and minimum suction-air velocities v_{min} of 2, 4, 8, and 12 feet per second.

The computed section power drag coefficients are presented in figure 24. Examination of this figure indicates that for the wing of this investigation at a section lift coefficient of 1.71, minimum power

for a given v_{min} would be obtained with materials having the following porosity characteristics:

v_{min} (fps)	Index of resistivity, τ
2	7.6
4	4.0
8	1.4
12	1.1

As the v_{min} is increased, the index of resistivity necessary for minimum power decreases. For a given v_{min}, materials with indices of resistivity lower than that for minimum power show a quite rapid rise in the power required. Materials with higher indices do not show as rapid an increase in power required but the pressure ratios (p_o/p_1) are excessively large. For a section lift coefficient of 1.44, the values of τ for minimum power were about the same as for a lift coefficient of 1.71.

The experimental data for the wing with constant thickness of material 1 (configuration A), presented in figures 13 and 14, indicate that satisfactory lift characteristics were obtained with a v_{min} of 4 feet per second. From figure 24 it can be seen that minimum power for a v_{min} of 4 feet per second, using a constant thickness of material as the porous surface, was approached quite closely in the tests with material 1 having a τ of 7.0. For the conditions of the tests, that is, v_{min} of 4 feet per second, lift coefficient of 1.71, q_o of 30 pounds per square foot, and chord of 4.5 feet, the power drag coefficient for configuration A was 0.033 which corresponds to a horsepower per foot of span of 1.3. At the v_{min} of 5 feet per second necessary to obtain a lift coefficient of 1.71 with configuration B, which had a more dense material for the porous area, the power drag coefficient was 0.064 which corresponds to a horsepower per foot of span of 2.5.

Variable Resistivity

For a uniformly porous material the chordwise distribution of resistivity of the material may be varied by stepping or tapering the thickness of the material. Numerous chordwise distributions of suction-air velocity are possible, depending on the distribution and resistivity of the material used. The variables involved affect the suction pressure required as well as the chordwise distribution of suction-air velocity. Possible reduction in power depends upon the attainment of satisfactory lift characteristics with the resulting suction-air-velocity distribution. In addition, the physical size of the wing section imposes restrictions on the thickness of the material required to give a desired velocity distribution.

In order to illustrate the change in power resulting from a change in chordwise distribution of the index of resistivity τ of the material, calculations were made for an assumed section lift coefficient of 1.71 and a v_{min} of 5 feet per second for various chordwise distributions of thickness of material 7 of table I. The index of resistivity τ of this material is 3.6 which is approximately the resistivity necessary for minimum suction power for a v_{min} of 5 feet per second with a constant thickness of material. The arrangements for which computations were made are shown in figure 25 with the corresponding suction-air-velocity diagrams. The power drag coefficients c_w for these arrangements are tabulated below:

Velocity distribution	c_w
(a) Increasing from L.E. to 0.03c (constant τ)	0.029
(b) Constant velocity	.020
(c) Decreasing from L.E. to 0.03c	.015

It is apparent that power drag coefficients can be calculated for various taper arrangements between (a) and (c) of figure 25 as well as tapered thicknesses greater than (c). Power drag coefficients also can be calculated using materials of porosities different from that of material 7. If these materials were tapered to match the suction velocity diagrams in figure 25, the resulting power drag coefficients would then be dependent on the plenum chamber pressures which are a function of the resistivity of the material. Thus materials other than 7 and thickness distributions other than those discussed above could be used which would give power drag coefficients greater or less than those shown for material 7. A practical limitation of the porous material itself must be considered if usable values of suction power are to be obtained. The limitation would be sufficient thickness for strength at the leading edge of the suction area without excessive thickness at the rearmost point of area suction. This limitation, applicable to porous materials of uniform resistivity, could be overcome if porous materials of varying resistivity for a constant thickness were available.

The resistivity of the material also may be varied chordwise by stepping the thickness of the material as was done for configuration C (fig. 2). As a multistep arrangement would approach that of the tapered arrangement, the same discussion as applied to the tapered materials will in general apply to the stepped arrangements. The experimental data in figure 14 show that satisfactory lift characteristics were obtained with configuration C for a v_{min} of 5 feet per second. For the conditions of the test, that is, v_{min} of 5 feet per second, lift coefficient of 1.7, q_o of 30 pounds per square foot, and chord of 4.5 feet, the power drag

coefficient was 0.024 which corresponds to a horsepower per foot of span of 0.96.

Power drag coefficients lower than those given above may be possible with materials and distributions of resistivity other than those illustrated in figures 2 and 25. Again, the minimum power attainable is governed by the suction-air velocity necessary to obtain satisfactory lift characteristics at a given free-stream velocity.

CONCLUDING REMARKS

The maximum lift of the symmetrical 10.51-percent-thick wing was increased from a lift coefficient c_l of approximately 1.3 to approximately 1.8 by means of area suction over the first 3 percent of chord for a section flow coefficient of 0.0014 at a free-stream dynamic pressure of 30 pounds per square foot.

The maximum lift of the plain wing appeared to be limited by leading-edge stall, whereas the stall of the wing with suction appeared to result from separation of the turbulent boundary layer from the trailing edge. This would make subsequent increases in the maximum lift dependent on control of the turbulent boundary layer.

The flow-resistance characteristics as well as the chordwise variation of permeability were found to be important in reducing the suction-flow quantity and suction power required for a given lift. A c_l of 1.71 was attained with a c_Q of 0.00135 and a power drag coefficient c_w of 0.033 with a porous surface material of constant resistivity. By stepping the thickness of the porous material and hence changing the chordwise distribution of resistivity, the c_Q required to attain a c_l of 1.71 was reduced to 0.0008 and c_w was reduced to 0.024.

An analysis of the effects of the distribution and resistivity of the porous surface material on the suction power and velocity distribution indicated that power drag coefficients lower than those obtained in the tests may be possible. It must be emphasized, however, that the minimum power attainable will be governed by the suction-air velocities necessary to obtain satisfactory lift characteristics at a given free-stream velocity.

Ames Aeronautical Laboratory
National Advisory Committee for Aeronautics
Moffett Field, Calif., Sept. 30, 1952.

APPENDIX

DETERMINATION OF SECTION POWER DRAG COEFFICIENT

In deriving an expression for the suction power in terms of the test variables P_1, c_Q and q_o, it was assumed that the air is a perfect gas with a value of $\gamma = 1.4$, the absolute pressure at sea level is 2116 pounds per square foot, and the dynamic head of suction air was negligible. Ducting and compressor losses were neglected.

The power required of a compressor to pump the suction air back to free-stream static pressure can be estimated for single-stage adiabatic compression (see reference 11) by means of the following expression:

$$\text{Power} = \left(\frac{\gamma}{\gamma-1}\right) Q_1 p_1 \left[\left(\frac{p_o}{p_1}\right)^{\frac{\gamma-1}{\gamma}} - 1\right] \tag{1}$$

In order to express the power in a form more comparable to the aerodynamic coefficients, the power required for suction can be written in terms of a power drag coefficient, that is, the drag equivalent of the suction power:

$$c_w = \frac{1}{c q_o U_o} \left(\frac{\gamma}{\gamma-1}\right) Q_1 p_1 \left[\left(\frac{p_o}{p_1}\right)^{\frac{\gamma-1}{\gamma}} - 1\right] \tag{2}$$

By assuming a constant temperature throttling process as the air passes through the porous material, Q_1 in the above equation may be expressed in terms of the coefficient c_Q. From the equation of continuity

$$Q = c_Q U_o c \frac{\int p_e ds}{p_1 \int ds} \tag{3}$$

where the limits of integration are the foremost and rearmost points of area suction. The evaluation of equation (3) may be simplified by assuming that

$$\frac{\int p_e ds}{\int ds} = p_o \tag{4}$$

Hence,

$$Q_1 = c_Q U_o c \frac{p_o}{p_1} \tag{5}$$

approximately.

Using the relationship

$$P_1 = \frac{p_1 - p_o}{q_o} \tag{6}$$

and substituting equation (5) into equation (2) and expanding the resulting expression in a power series, the section power drag coefficient for low subsonic Mach numbers can be expressed in terms of the test variables as

$$c_w = -c_Q P_1 \left\{ 1 + \frac{(1-2\gamma)}{2!\gamma} \frac{P_1 q_o}{p_o} + \frac{(1-2\gamma)(1-3\gamma)}{3!\,\gamma^2} \left(\frac{P_1 q_o}{p_o} \right)^2 + \cdots + \left[\frac{(1-2\gamma)(1-3\gamma) \cdots 1-(n+1)\gamma}{(n+1)!\,\gamma^n} \right] \left(\frac{P_1 q_o}{p_o} \right)^n + \cdots \right\} \tag{7}$$

where $\frac{P_1 q_o}{p_o}$ is less than unity.

A solution of equation (7) is presented in figure 26 for a dynamic pressure of 30 pounds per square foot. In figure 27, the ratio of c_w to the quantity $-c_Q P_1$ is presented as a function of the dynamic pressure for various values of the suction pressure coefficient.

REFERENCES

1. Thomson, K. D.: A Review of Leading Edge High Lift Devices. Australian Aero. Res. Lab., Dept. of Supply. Rep. A77, June 1951.

2. McCullough, George B., and Gault, Donald E.: An Experimental Investigation of an NACA 63_1-012 Airfoil Section with Leading-Edge Suction Slots. NACA TN 1683, 1948.

3. Nuber, Robert J., and Needham, James R., Jr.: Exploratory Wind-Tunnel Investigation of the Effectiveness of Area Suction in Eliminating Leading-Edge Separation over an NACA 64_1A212 Airfoil. NACA TN 1741, 1948.

4. Preston, J. H.: The Boundary-layer Flow over a Permeable Surface through which Suction is Applied. R. & M. No. 2244, British A. R. C., 1946.

5. Thwaites, B.: A Theoretical Discussion of High-Lift Aerofoils with Leading-Edge Porous Suction. R. & M. No. 2242, British A. R. C., 1946

6. Muskat, Morris: The Flow of Homogeneous Fluids through Porous Media. J. W. Edwards, Inc., Ann Arbor, Mich., 1946.

7. Iberall, Arthur S.: Permeability of Glass Wool and Other Highly Porous Media. Research Paper 2150, Jour. of Res., National Bureau of Standards, vol. 45, no. 5, November 1950.

8. Allen, H. Julian, and Vincenti, Walter G.: Wall Interference in a Two-Dimensional-Flow Wind Tunnel, with Consideration of the Effect of Compressibility. NACA Rep. 782, 1944.

9. McCullough, George B., and Gault, Donald E.: Examples of Three Representative Types of Airfoil-Section Stall at Low Speed. NACA TN 2502, 1951.

10. von Doenhoff, Albert E., and Tetervin, Neal: Determination of General Relations for the Behavior of Turbulent Boundary Layers. NACA Rep. 772, 1943.

11. Young V. W., and Young, Gilbert A.: Elementary Engineering Thermodynamics. McGraw-Hill Book Co., New York, 1941.

12. Anon.: Filter Paper, The Eaton-Dikeman Company, Mount Holly Springs, Pennsylvania, 1950.

13. Anon.: Catalog No. 70, American Filter Papers, Carl Schleicher and Schuell Co., New York 1949.

14. Anon.: Porex, Moraine Products, General Motors Corporation, Dayton, Ohio, 1943.

15. Anon.: Wel-Met Specifications MS-804, The Wel-Met Co., Kent, Ohio, 1941.

16. Anon.: Catalogue B-44, Oilite Bearings and Parts, Amplex Division, Chrysler Corporation, Detroit, Mich., 1950.

17. Anon.: Bulletin 224, Wesgo Specifications, Western Gold & Platinum Works, Ceramic Division, San Francisco, Calif., 1950.

18. Anon.: Perforated Materials, General Catalog No. 62, The Harrington & King Perforating Company, Chicago, Ill., 1950.

19. Anon.: Lektromesh Specifications Sheet, The C. O. Jelliff Mfg. Corp., Southport, Conn., 1949.

20. Anon.: Data Sheet No. 5, The American Felt Company, Glenville, Conn., 1947.

21. Anon.: Properties of Aircraft Quality Porous Stainless Steel, Aircraft Porous Media, Inc., Glen Cove, N.Y.

TABLE I.- FLOW RESISTANCE CHARACTERISTICS OF POROUS MATERIALS

Material				Reference	Backed with screen	Nominal thickness (in.)	$\Delta h = \tau v \varphi$	
No.	Description						τ	φ
Filter paper								
1	Grade 954, single sheet			12	Yes	0.0065	7.00	1.275
2	Grade 952, single sheet			12	Yes	.007	15.2	1.395
3	Grade 950, single sheet			12	Yes	.007	58.5	1.389
1&2	Single sheets of grades 954 and 952			12	Yes	.0135	21.2	1.395
4	Grade 404			13	Yes	.0085	4.28	1.355
5	Grade sharkskin			13	Yes	.005	7.60	1.444
Sintered bronze								
6	Grade 3			14	No	0.156	5.95	1.127
7	MS-804			15	No	.062	3.60	1.184
8	Part No. R-8001			16	No	.031	24.9	1.385
End grain wood								
9	Oak			- -	Yes	0.25	7.60	1.598
10	Balsa			- -	Yes	.25	68.0	1.878
11	Mahogany			- -	Yes	.25	82.2	1.992
12	Birch			- -	Yes	.25	82.2	1.992
Ceramic								
13	Refractory slab			17	No	0.50	34.1	1.366
14	Plaster of Paris			- -	Yes	.125	40.0	1.0
Perforated metal sheet								
15	No. 0 staggered			18	No	0.021	0.009	1.915
16	No. 1/20 staggered			18	No	.031	.020	1.985
17	40 count, 0.013 in. hole size			19	No	.007	.006	1.649
18	65 count, 0.005 in. hole size			19	No	.006	.035	1.595
Felt cloth								
	Color	Lb per yd	Percentage Wool	Percentage Cotton				
19	Light gray	0.25	60	40	20	Yes	0.031	0.12	1.279
20	White	1.0	35	65	20	Yes	.125	.42	1.254
21	Dark gray	2.1	60	40	20	Yes	.250	.75	1.179
22	Dark gray	4.2	60	40	20	Yes	.500	1.25	1.287
23	Black	5.3	60	40	20	Yes	.625	1.01	1.246
24	White	8.4	100	0	20	Yes	.508	8.3	1.263
Drilled metal plate (0.028 dia. hole)								
25	Hole spacing, 0.125 x 0.10 in. staggered				- -	No	0.125	0.20	1.936
Sintered steel								
26	Grade E				21	No	1/16	4.3	1.253

NACA

TABLE II.- SYMMETRICAL AIRFOIL USED IN THE INVESTIGATION
[Percent airfoil chord]

(a) Coordinates

Station	Ordinate	Station	Ordinate
0	0	40	5.253
.5	1.08	45	5.164
.75	1.31	50	4.994
1.25	1.64	55	4.733
2.5	2.21	60	4.401
5	2.94	65	3.982
7.5	3.433	70	3.481
10	3.807	75	2.910
15	4.352	80	2.329
20	4.724	85	1.747
25	4.995	90	1.166
30	5.166	95	.583
35	5.255	100	0
L. E. radius: 1.304			

(b) Comparison with NACA 0010.51 airfoil

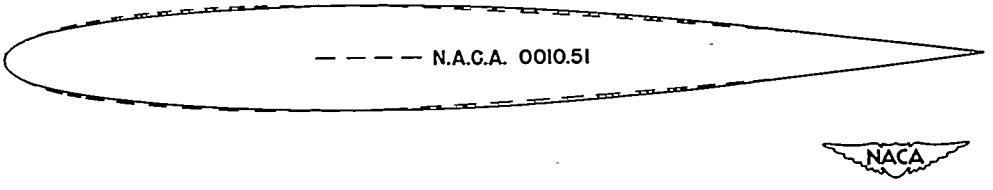

TABLE III.- END PLATE AND SLAT COORDINATES
[Percent airfoil chord]

(a) End plates (symmetrical about wing chord and 0.75 in. thick).

Station	Ordinate	Station	Ordinate
-33.3	0	88.9	44.4
-20	31.6	100	43.0
-10	39.1	110	39.1
0	43.0	120	31.6
11.1	44.4	133.3	0
50	44.4		

(b) Slat

Station	Ordinate		Station	Ordinate	
	Upper surface	Lower surface		Upper surface	Lower surface
-17.2	-4.71	-4.71	-12.0	-0.67	-0.67
-17.0	-3.93	-5.22	-8.0	.76	.76
-16.0	-2.82	-4.26	0	3.34	3.34
-15.0	-2.13	-2.98	5.7	5.19	5.19
-14.0	-1.59	-2.07			
-13.0	-1.08	-1.30			
			Center of L.E.R.	Station	Ordinate
				-16.7	-4.91
L.E.radius: 1.00					

Figure 1.- The 10.51-percent-thick symmetrical airfoil with a porous leading edge.

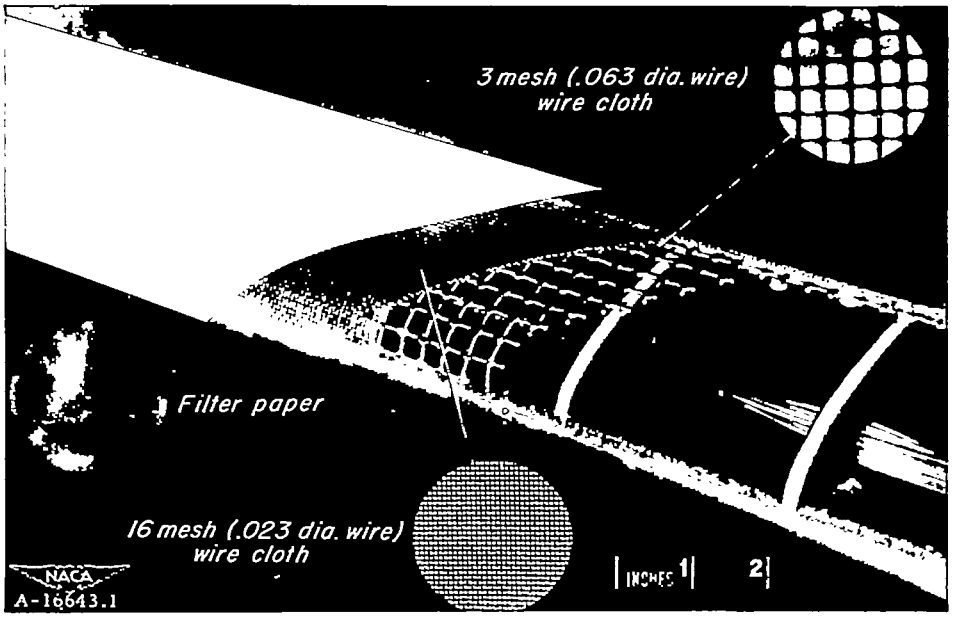

(a) Detail of porous leading-edge construction.

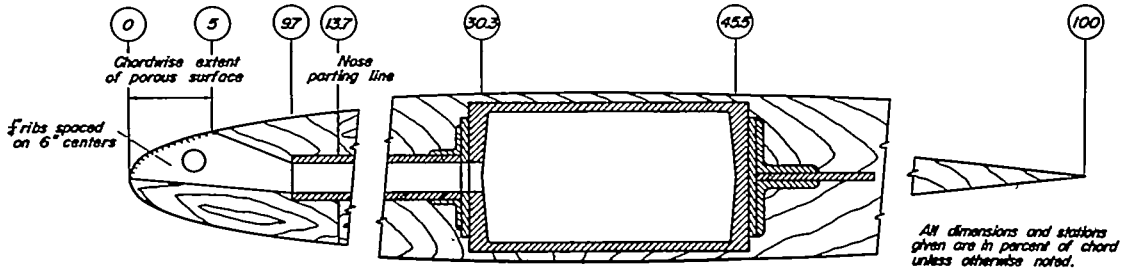

(b) Section through model with the nose block having a porous surface from 0 to 0.05c on the upper surface.

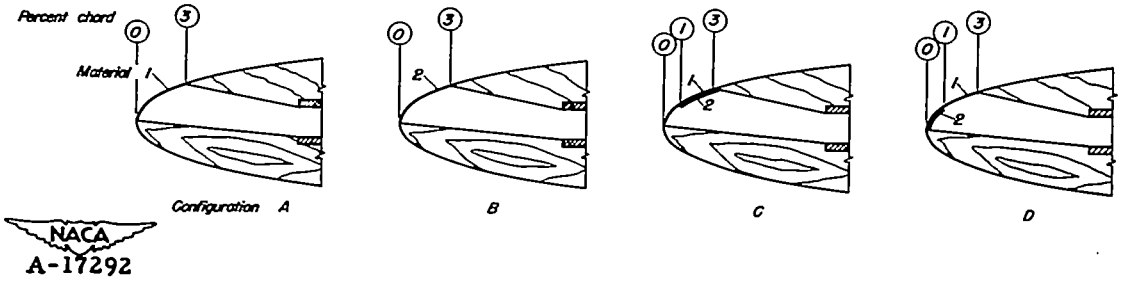

(c) The configurations tested with the nose section porous from 0 to 0.03c on the upper surface.

Figure 2.- Detail of the model construction and the porous leading-edge configurations tested.

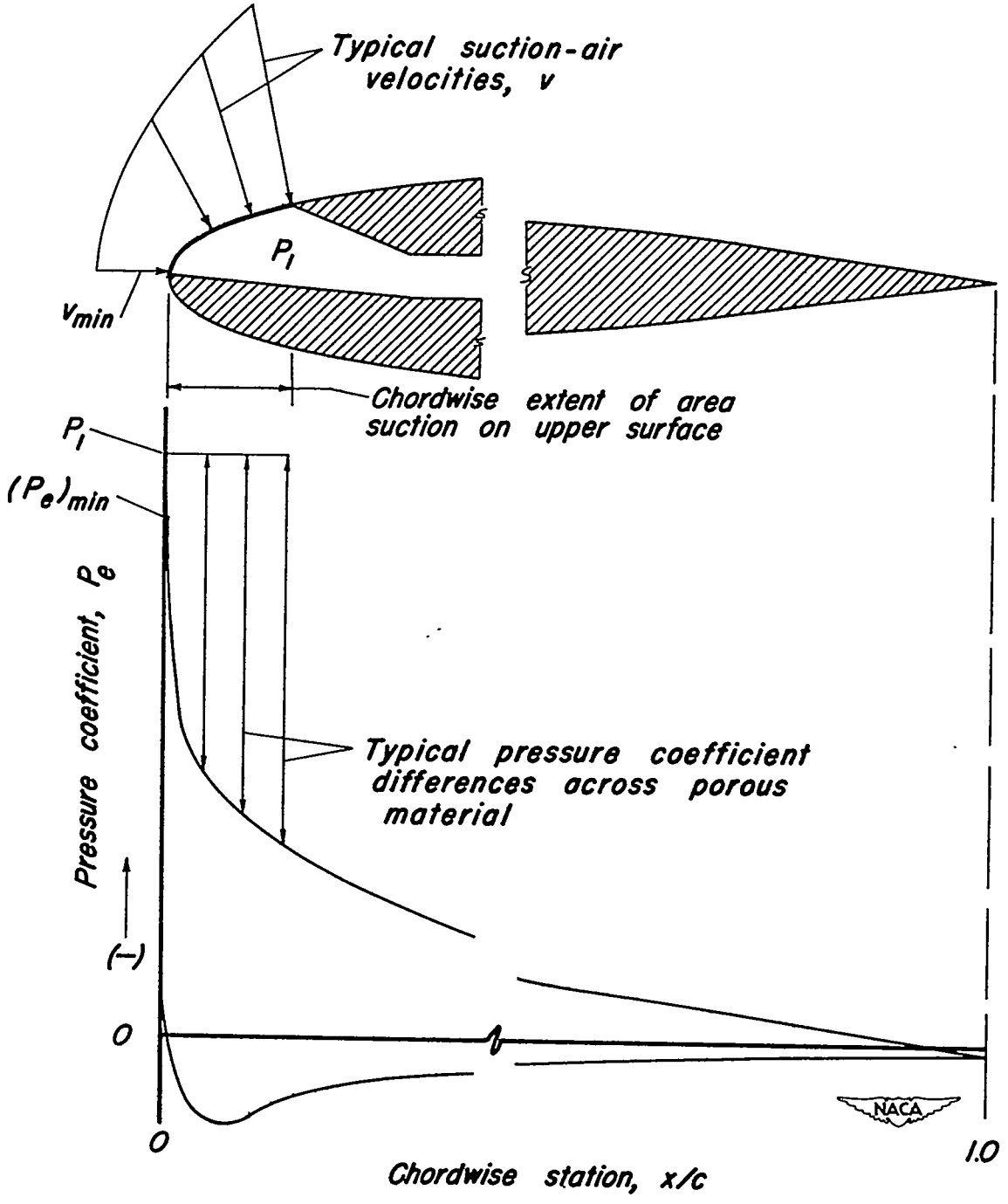

Figure 3.- Diagrammatic representation of the expressions used in determining the chordwise suction-air-velocity distribution.

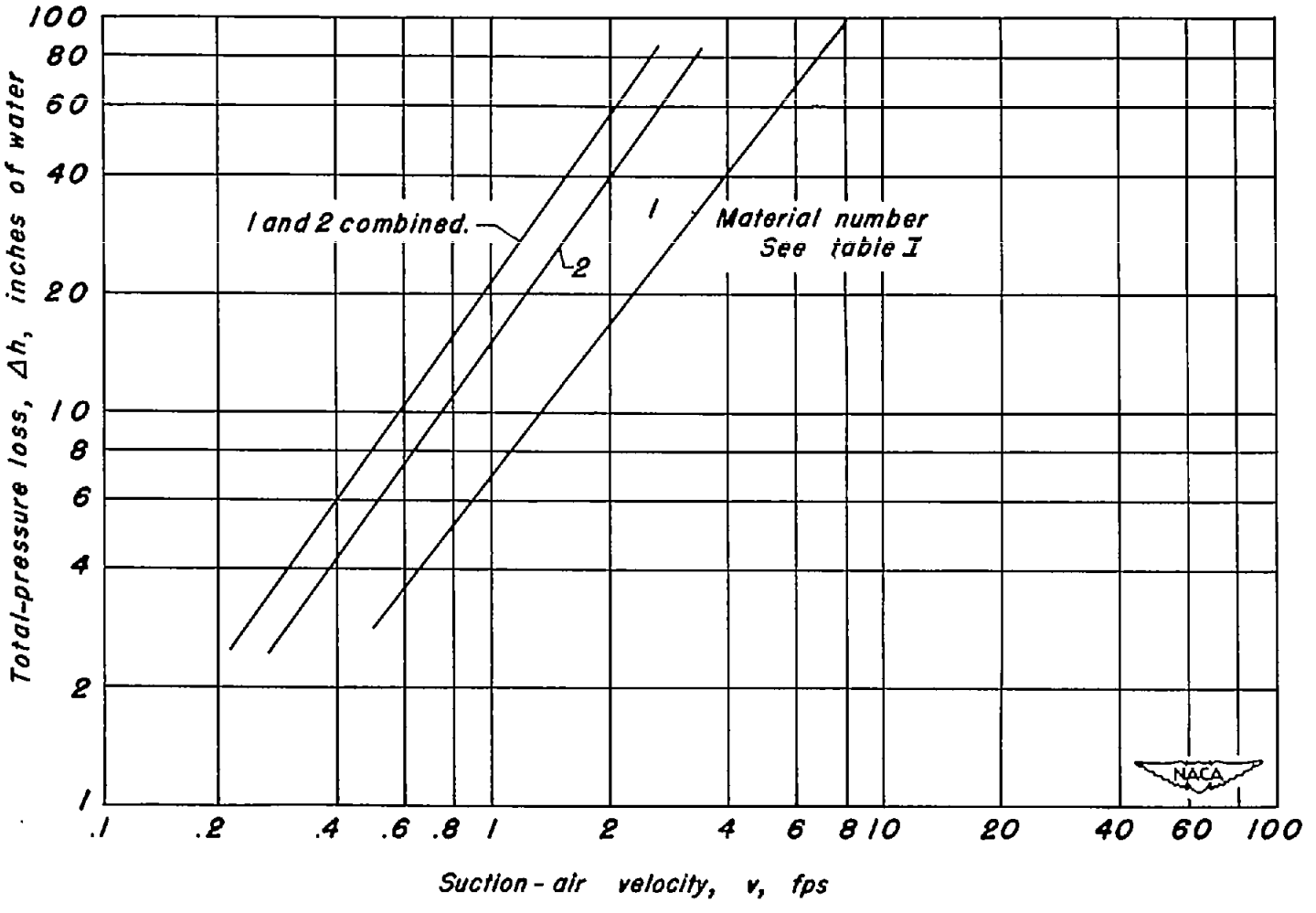

Figure 4.- Flow-resistance characteristics of the porous materials used in the tests.

(a) General arrangement of porous material sample and ASME orifice.

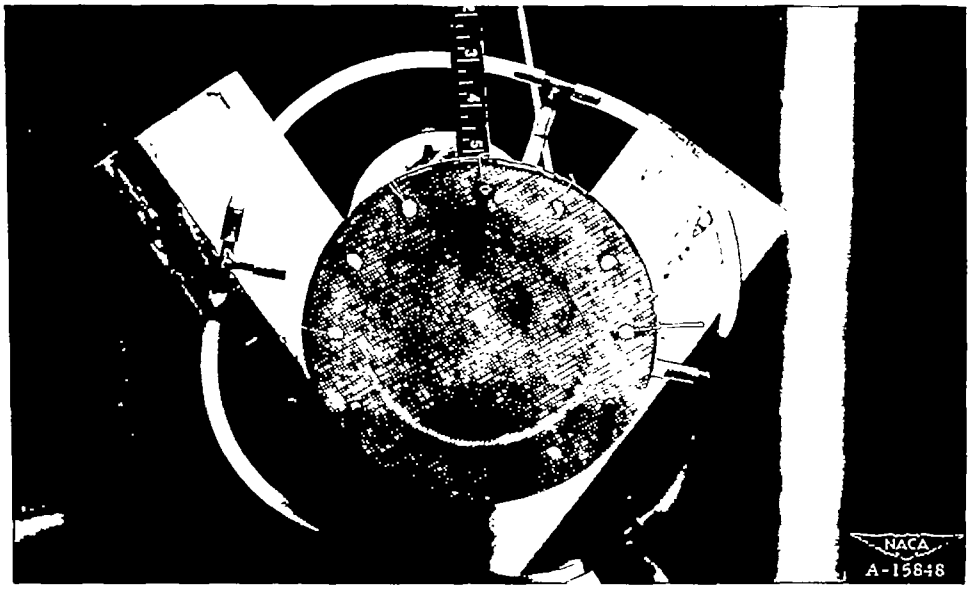

(b) The 16-mesh (0.023 diam. wire) wire cloth used for backing porous materials.

Figure 5.- Test setup for porous material calibration.

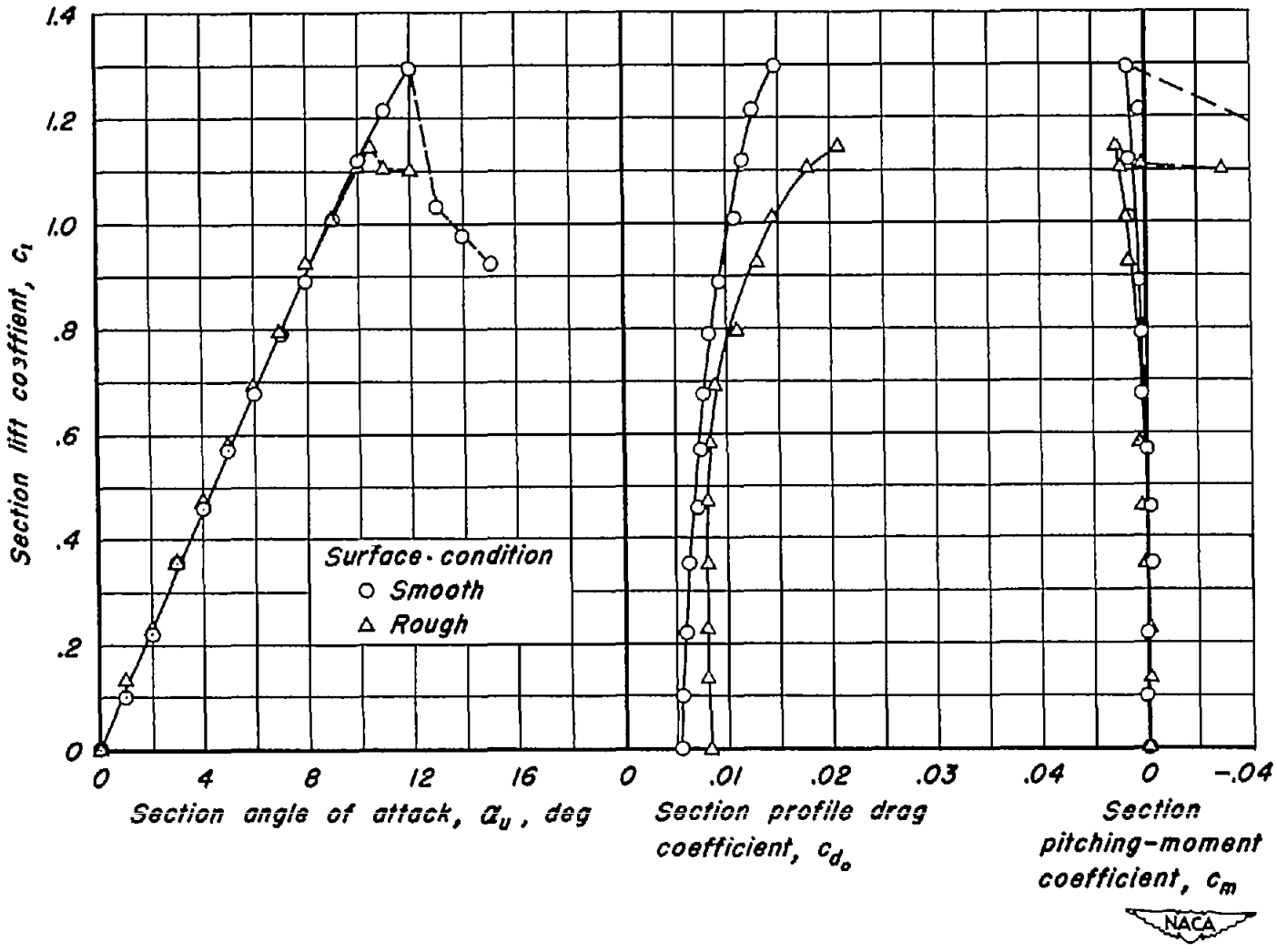

Figure 6.- Section aerodynamic characteristics of the plain wing for the smooth and rough surface conditions.

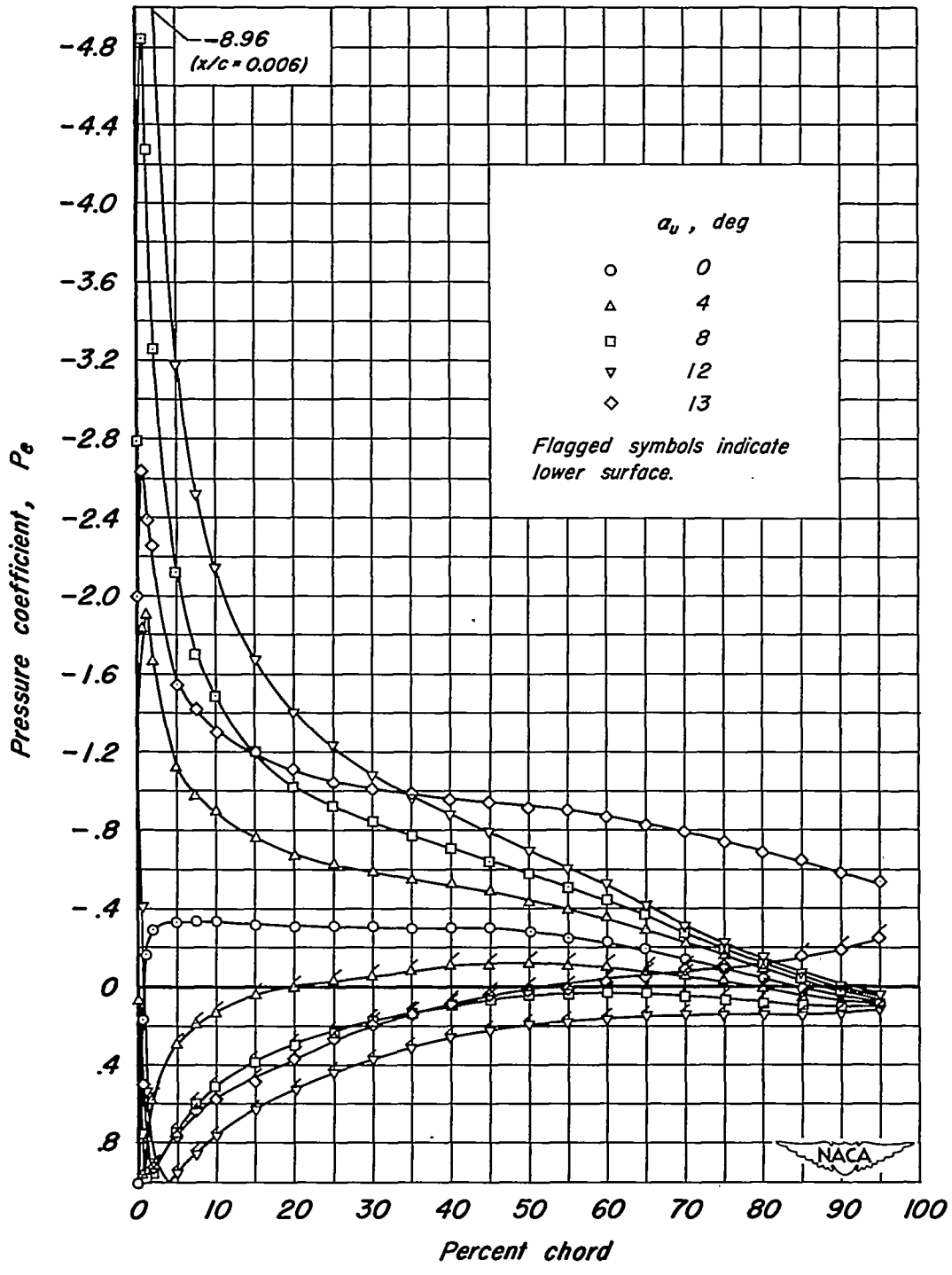

Figure 7.- Chordwise distribution of pressure over the plain wing for the smooth surface condition.

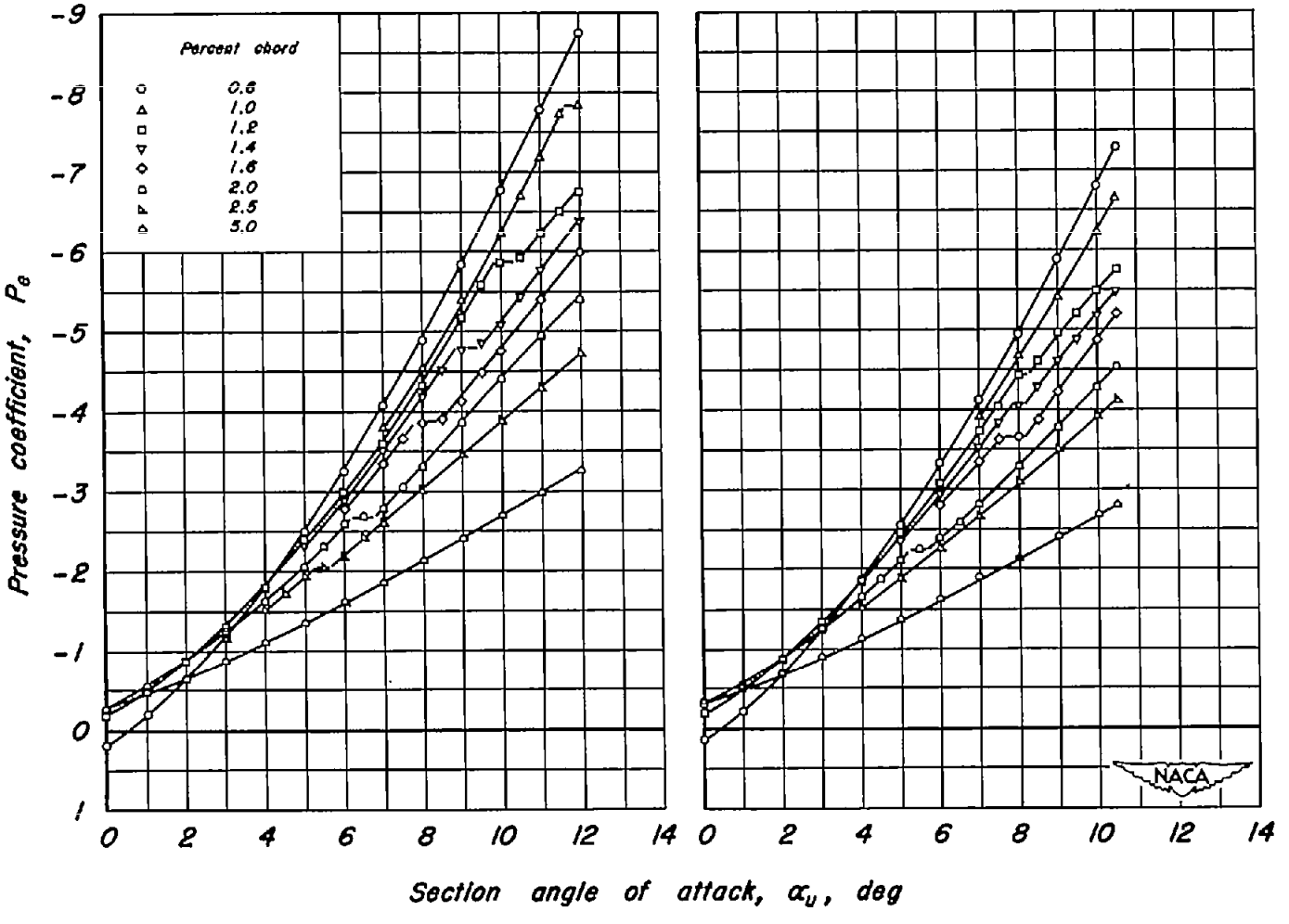

(a) Smooth surface condition. (b) Rough surface condition.

Figure 8.- Variation of pressure coefficient at particular chordwise stations with angle of attack for the plain wing.

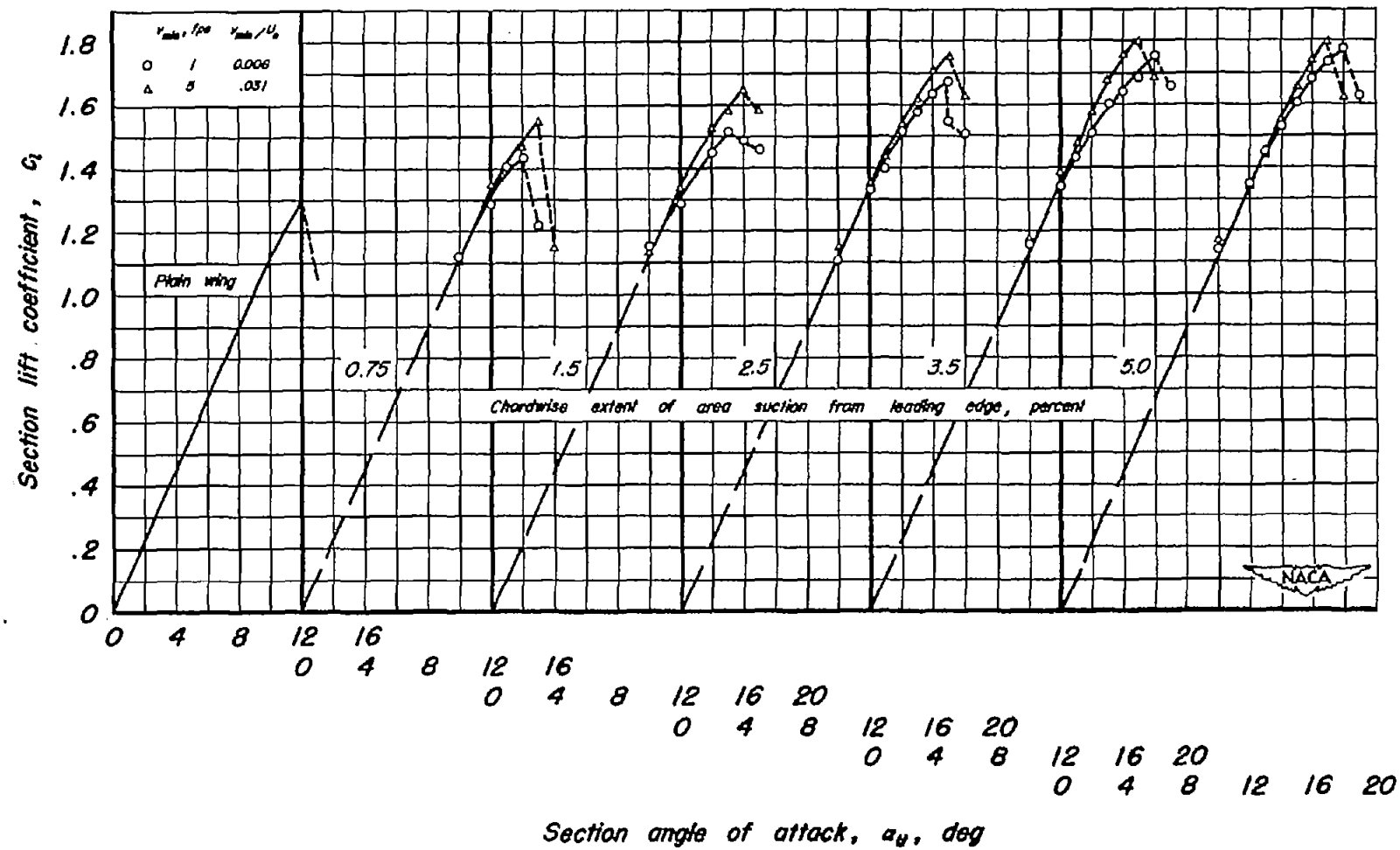

Figure 9.- Lift characteristics of the model for various chordwise extents of area suction.

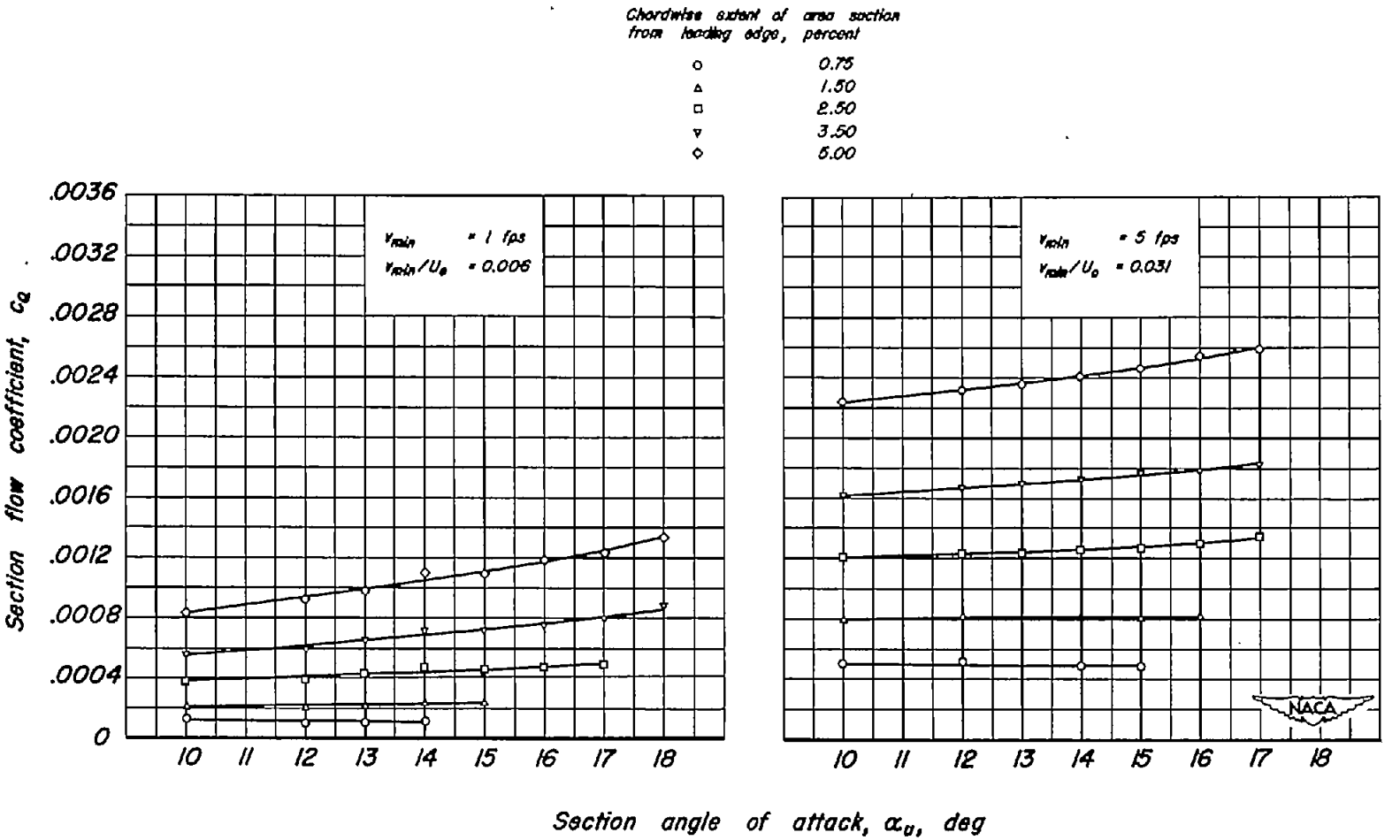

Figure 10.- Variation of section flow coefficient with angle of attack for various chordwise extents of area suction.

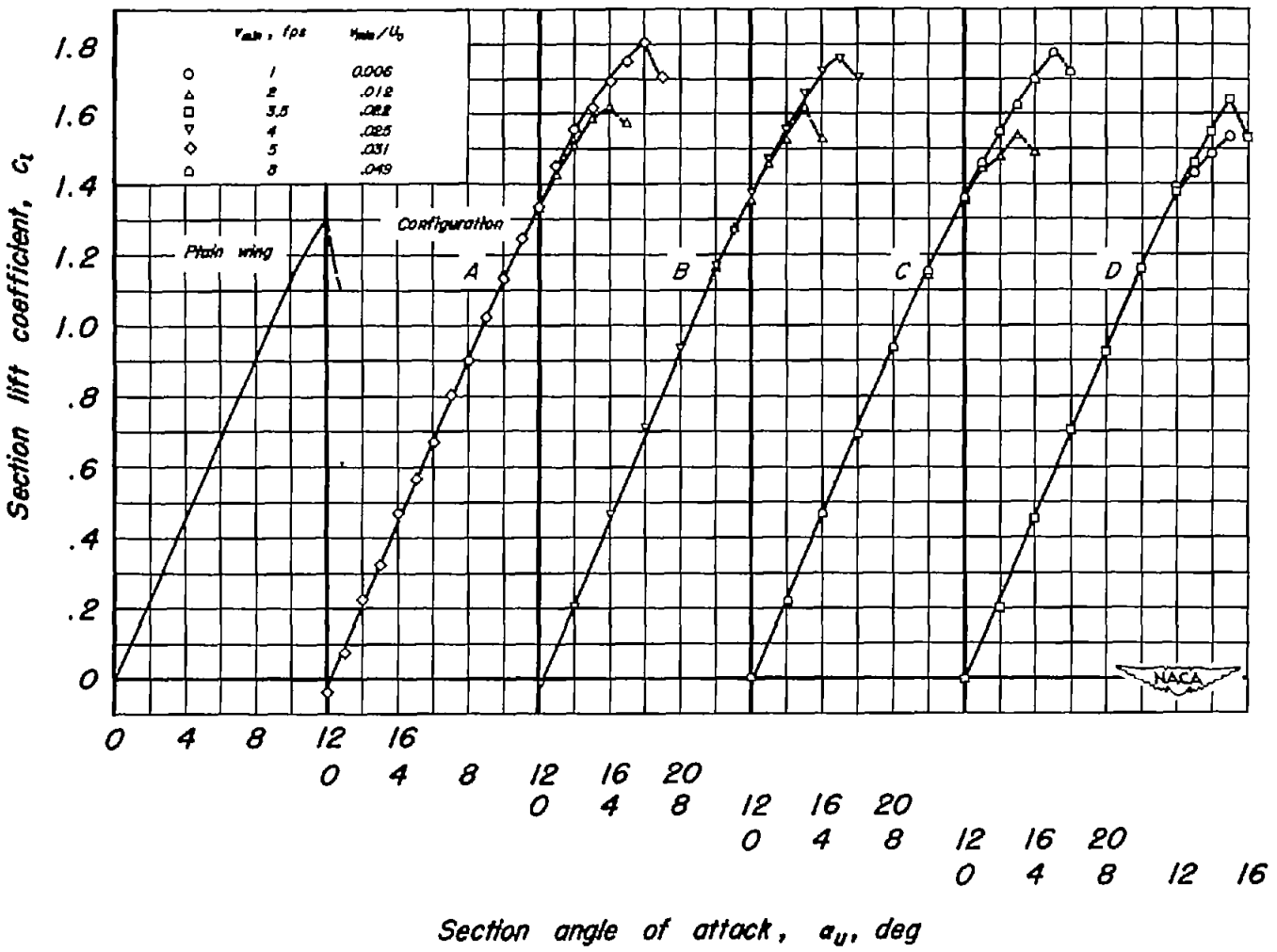

Figure 11.- Lift characteristics of the model for the various configurations tested. Chordwise extent of area suction from leading edge to 3-percent chord.

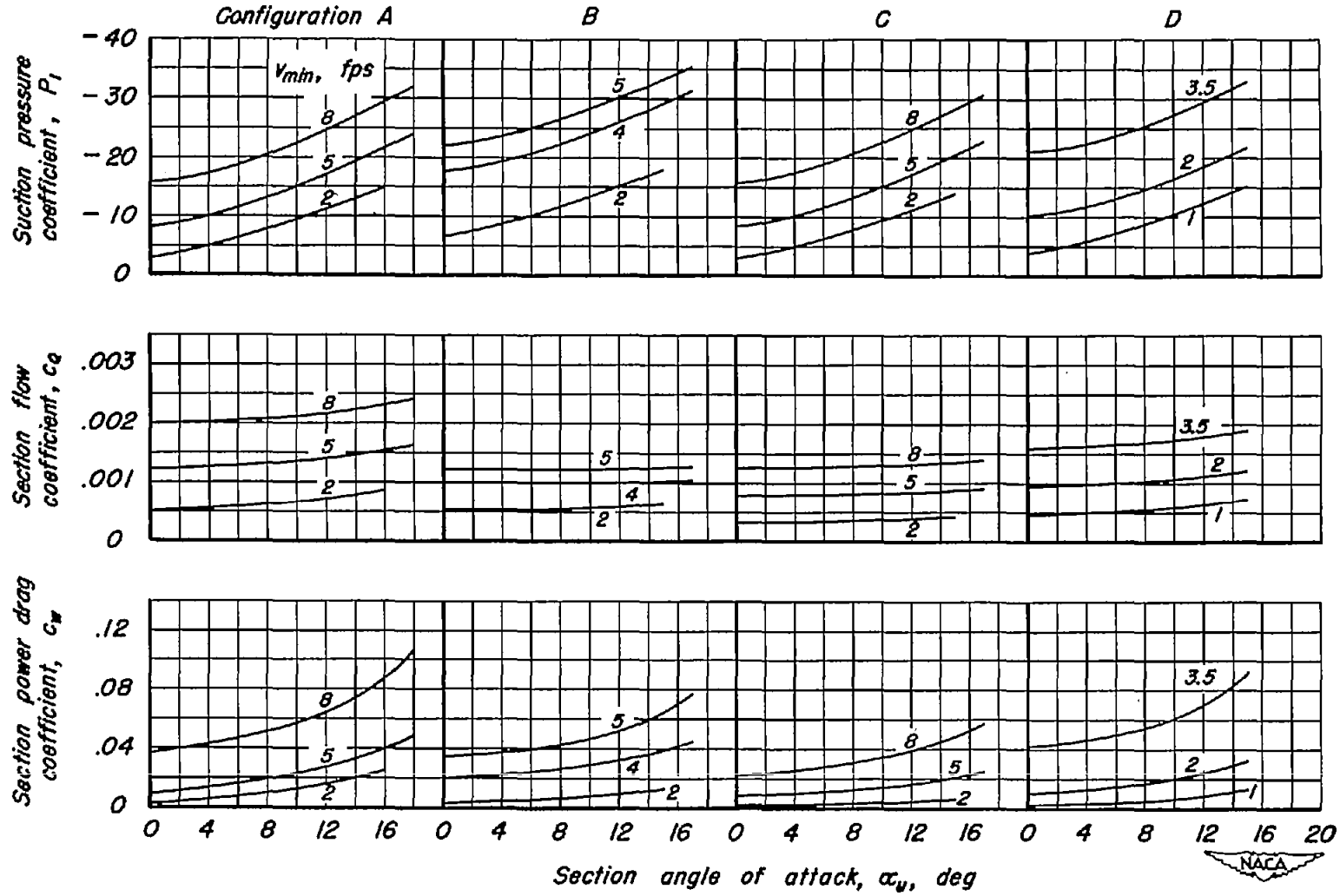

Figure 12.- Variation of the suction pressure, section flow, and section power drag coefficients with angle of attack for the various configurations tested.

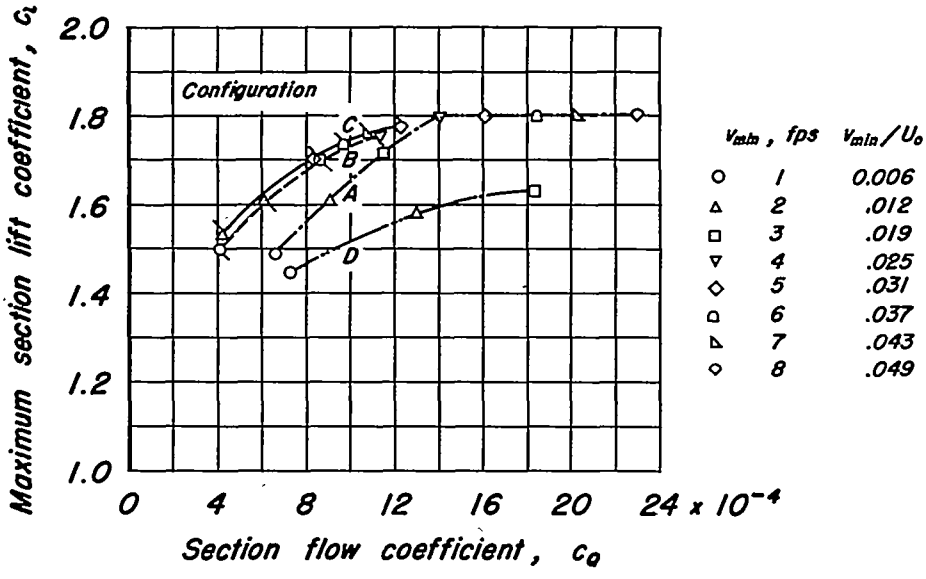

(a) Variation of maximum lift coefficient with flow coefficient.

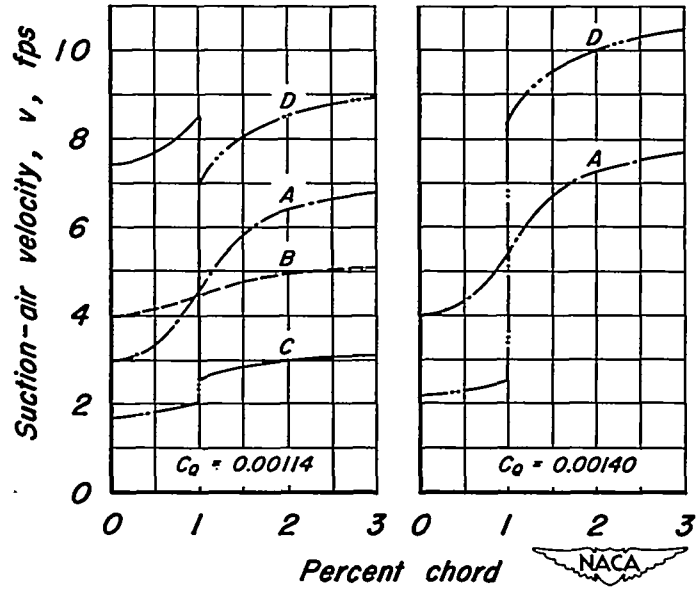

(b) Chordwise distributions of suction-air velocities.

Figure 13.- The effect of minimum suction velocity on the maximum lift for the various configurations tested.

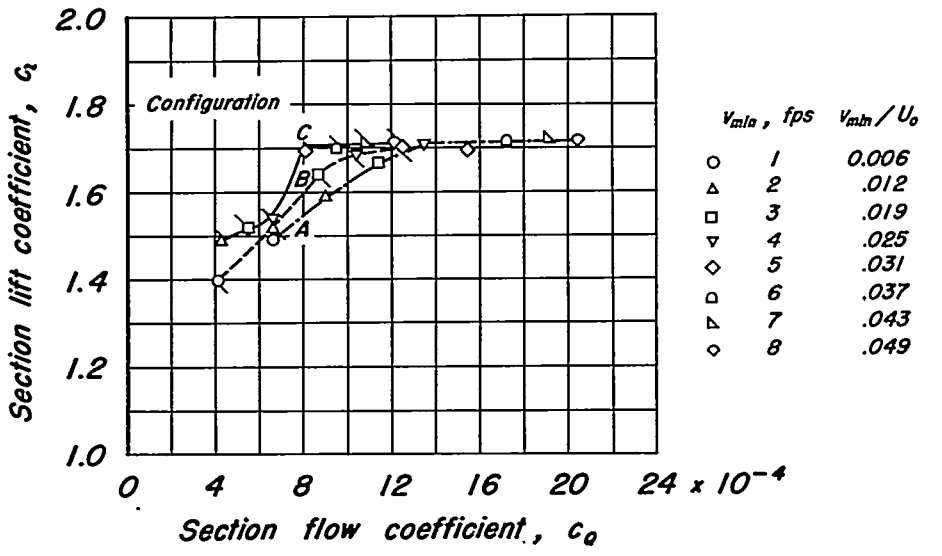

(a) Variation of lift coefficient with flow coefficient.

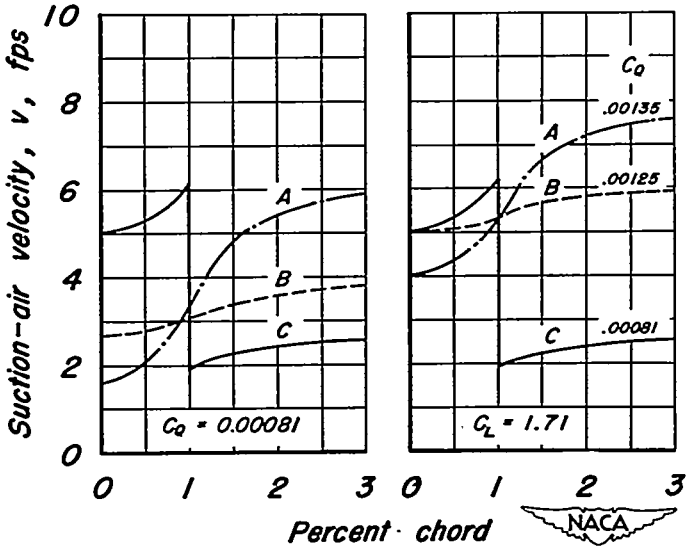

(b) Chordwise distributions of suction-air velocities.

Figure 14.- The effect of minimum suction velocity on the lift for an angle of attack of 16° for configurations A, B, and C.

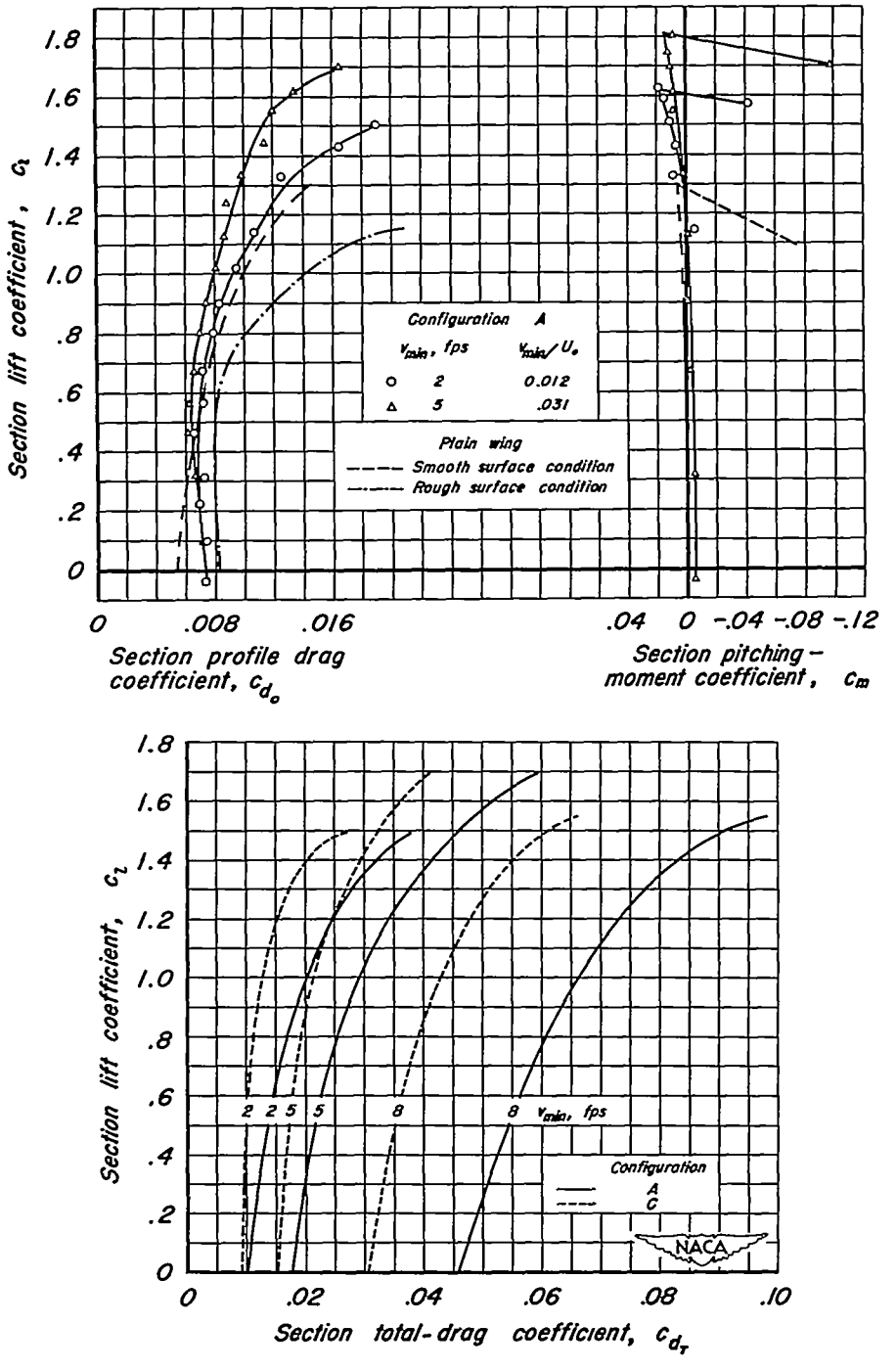

(a) Variation of drag and pitching moment with lift coefficient.

Figure 15.- Effect of suction on the drag and moment characteristics of the model.

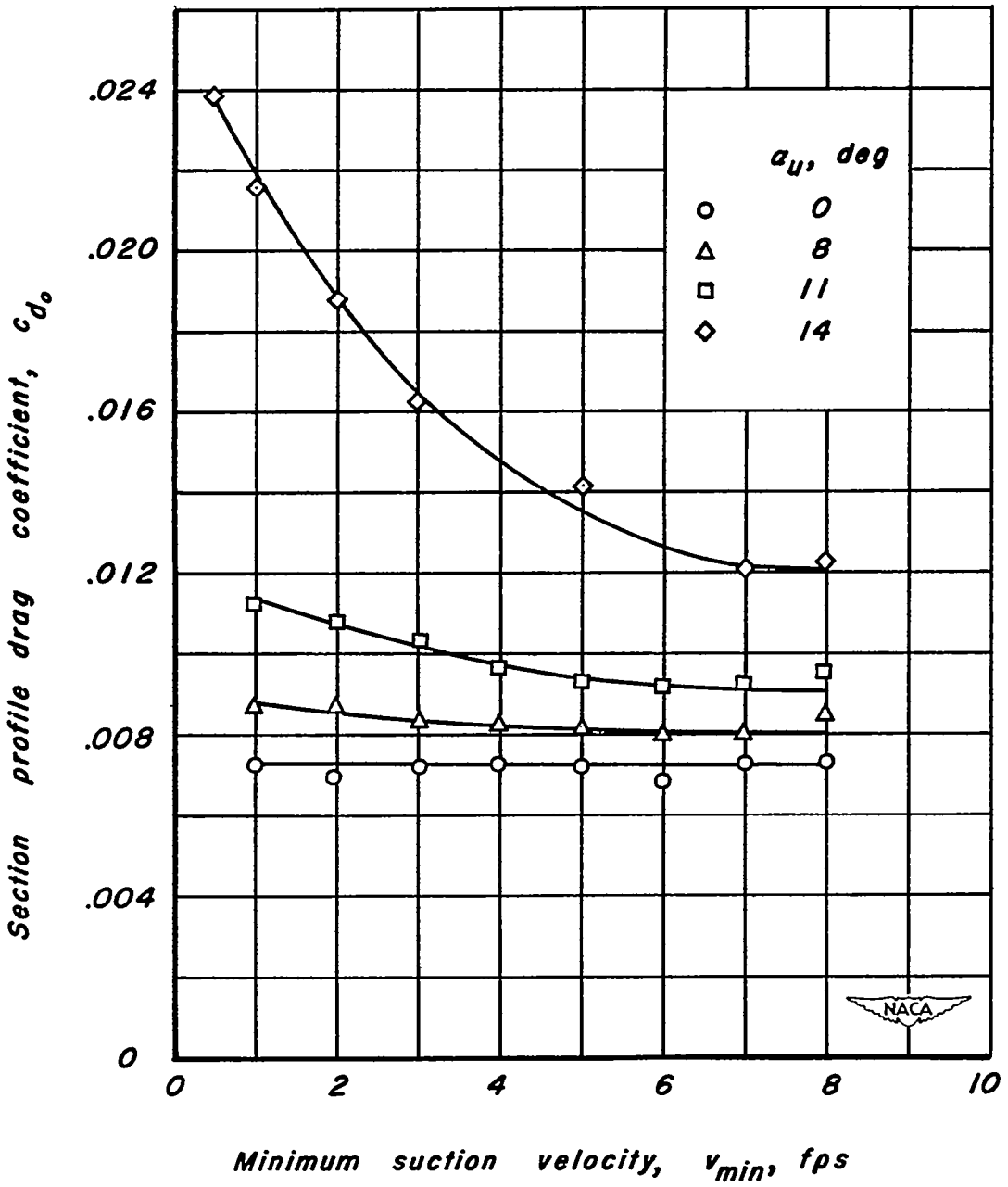

(b) Variation of profile drag coefficient with suction - air velocity. Configuration A.

Figure 15.- Concluded.

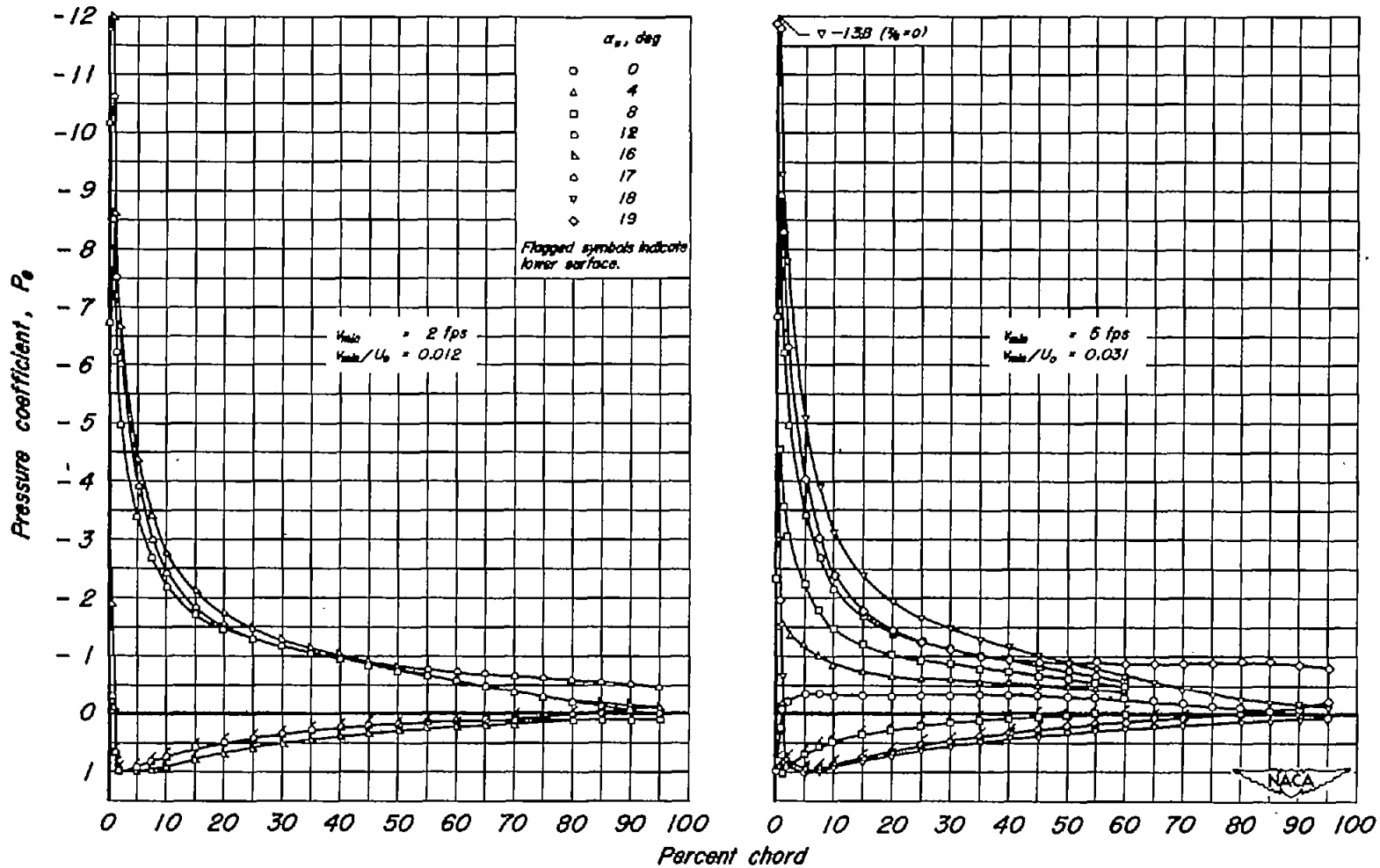

Figure 16.- Chordwise distribution of pressure over the model with configuration A.

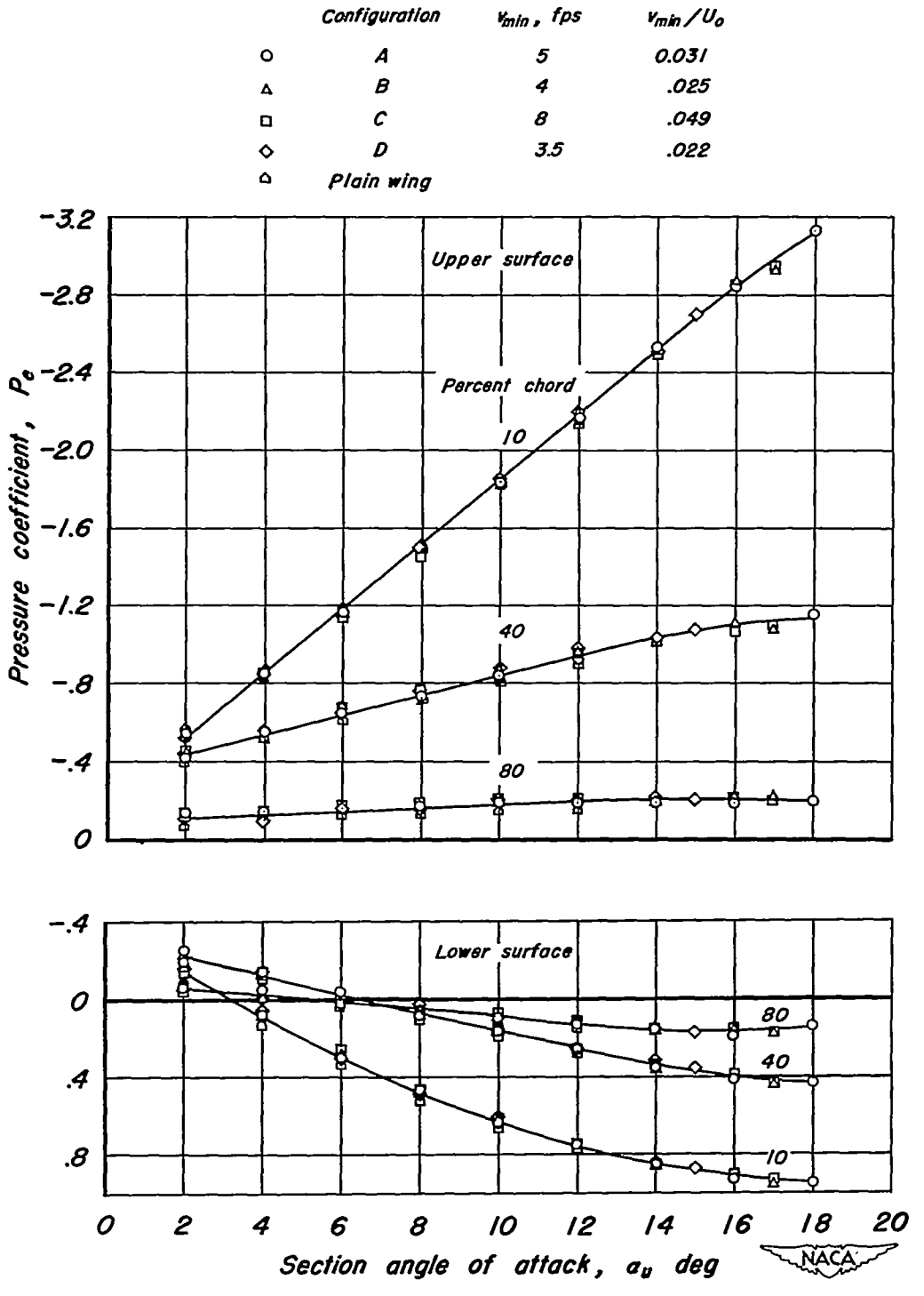

Figure 17.- Variation of the pressure coefficients at particular chordwise stations with angle of attack for the various configurations tested.

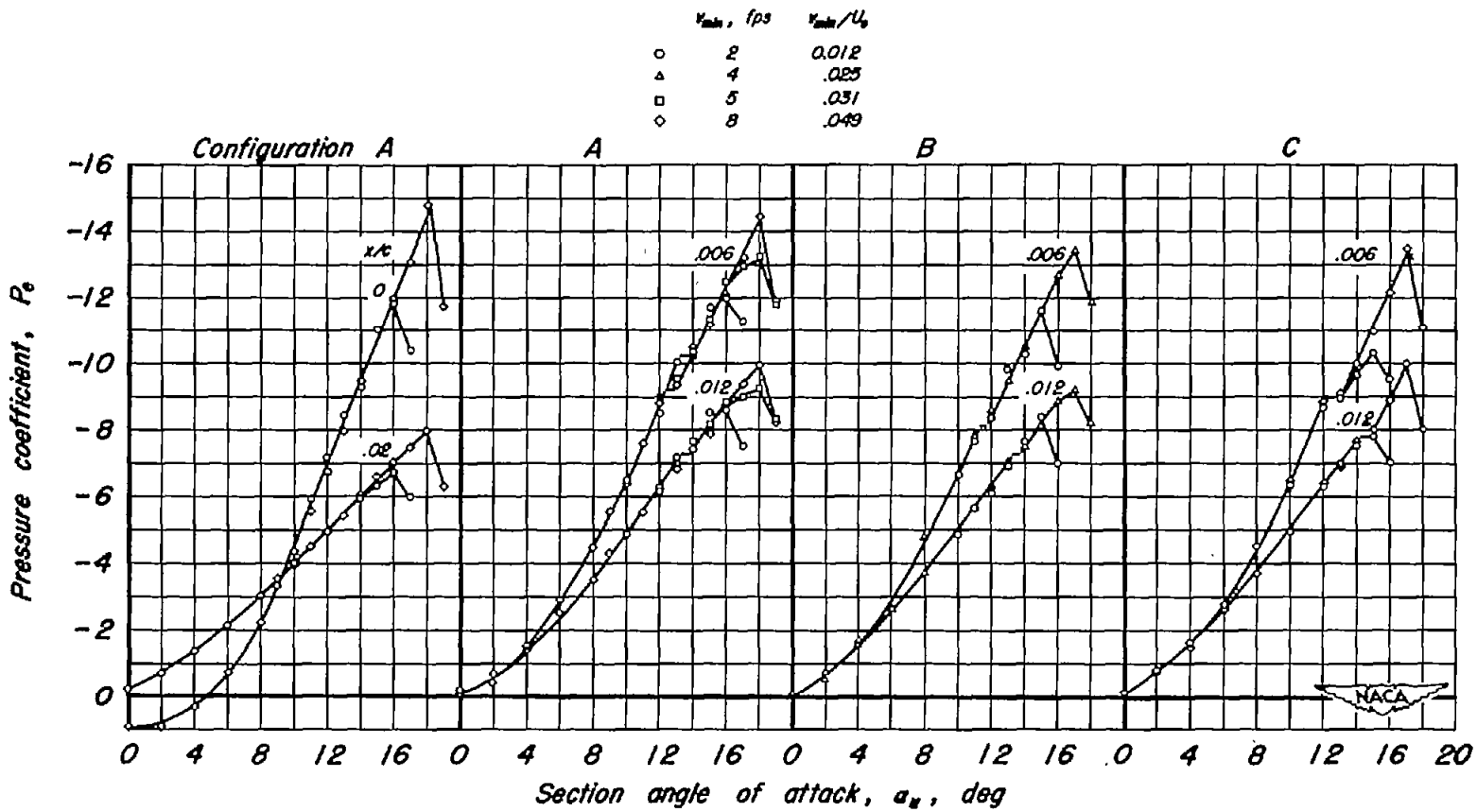

Figure 18.- Variation of pressure coefficients at particular chordwise stations with angle of attack for configurations A, B, and C.

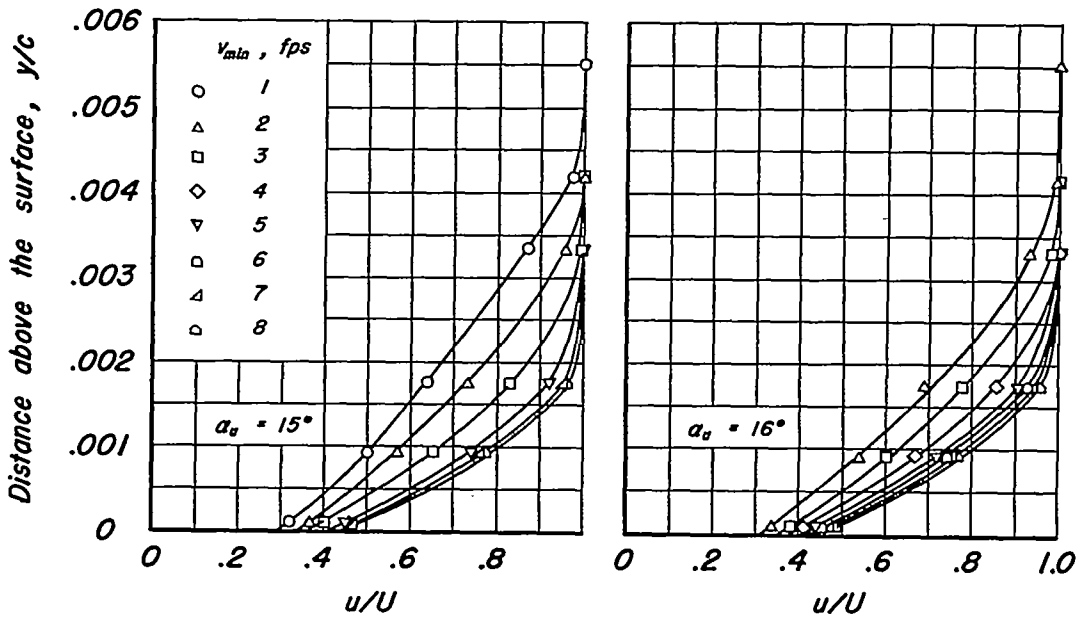

(a) Boundary-layer-velocity profiles at 0.10 chord.

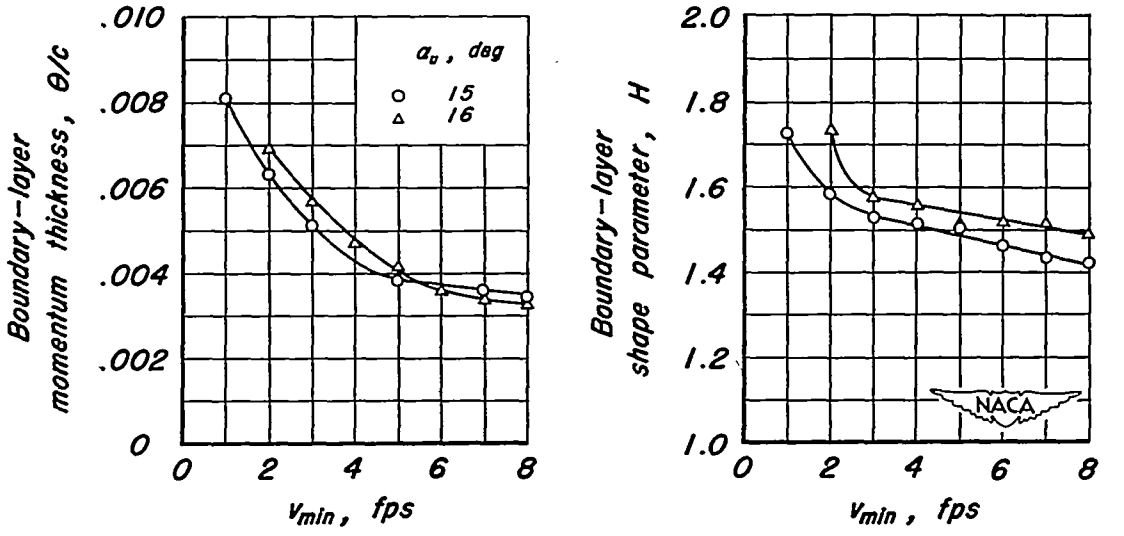

(b) Boundary-layer parameters.

Figure 19.- Boundary-layer characteristics at the 10-percent-chord station for angles of attack of 15° and 16° for the model with configuration A.

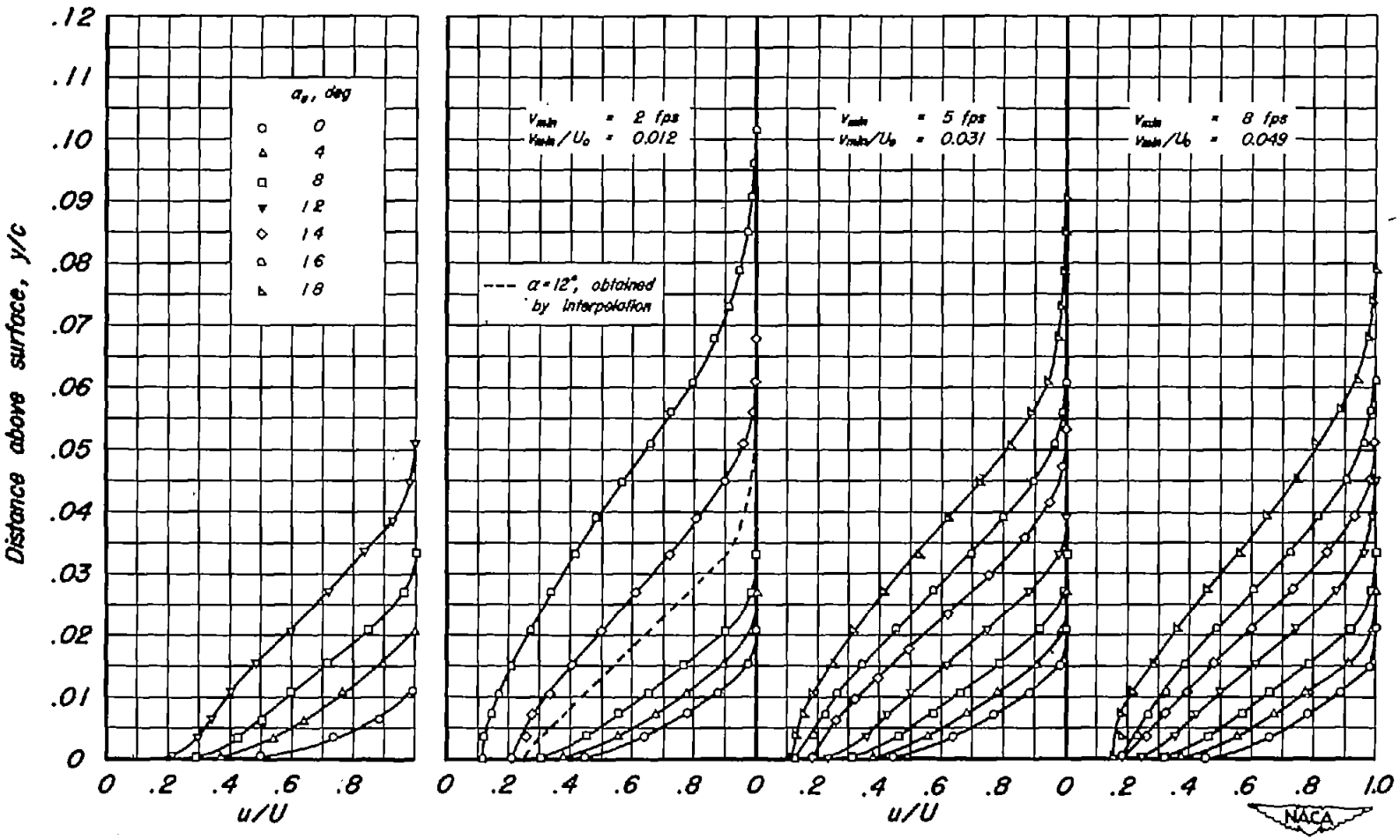

(a) Plain wing.

(b) Configuration A.

Figure 20.- Boundary-layer-velocity profiles at the 95-percent-chord station for the plain wing (smooth surface condition) and the model with configuration A.

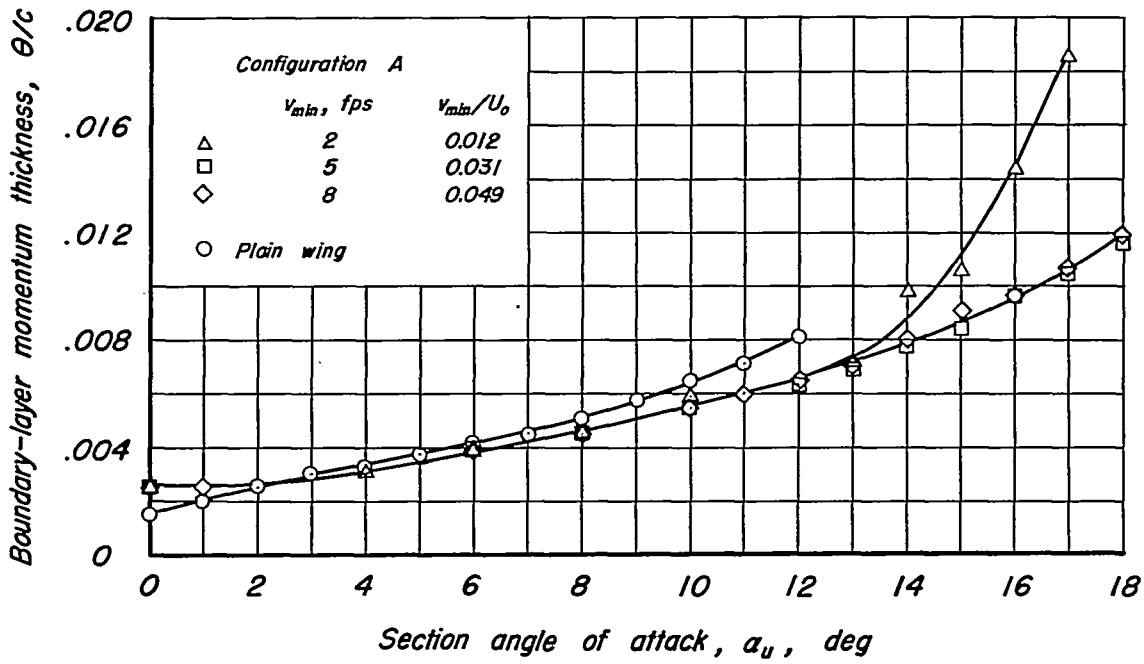

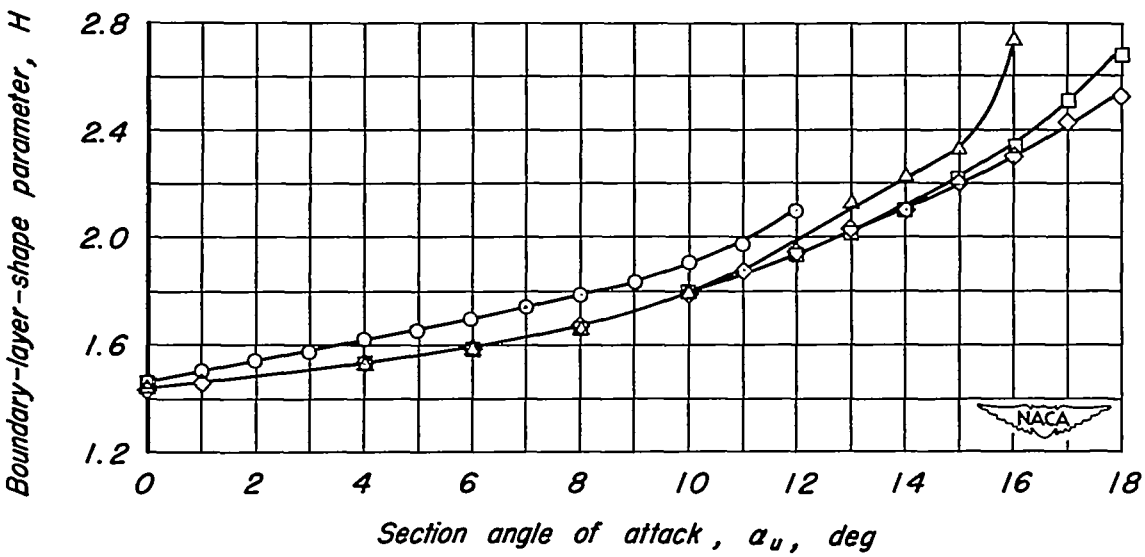

Figure 21.- Boundary-layer parameters at the 95-percent-chord station for the plain wing (smooth surface condition) and the model with configuration A.

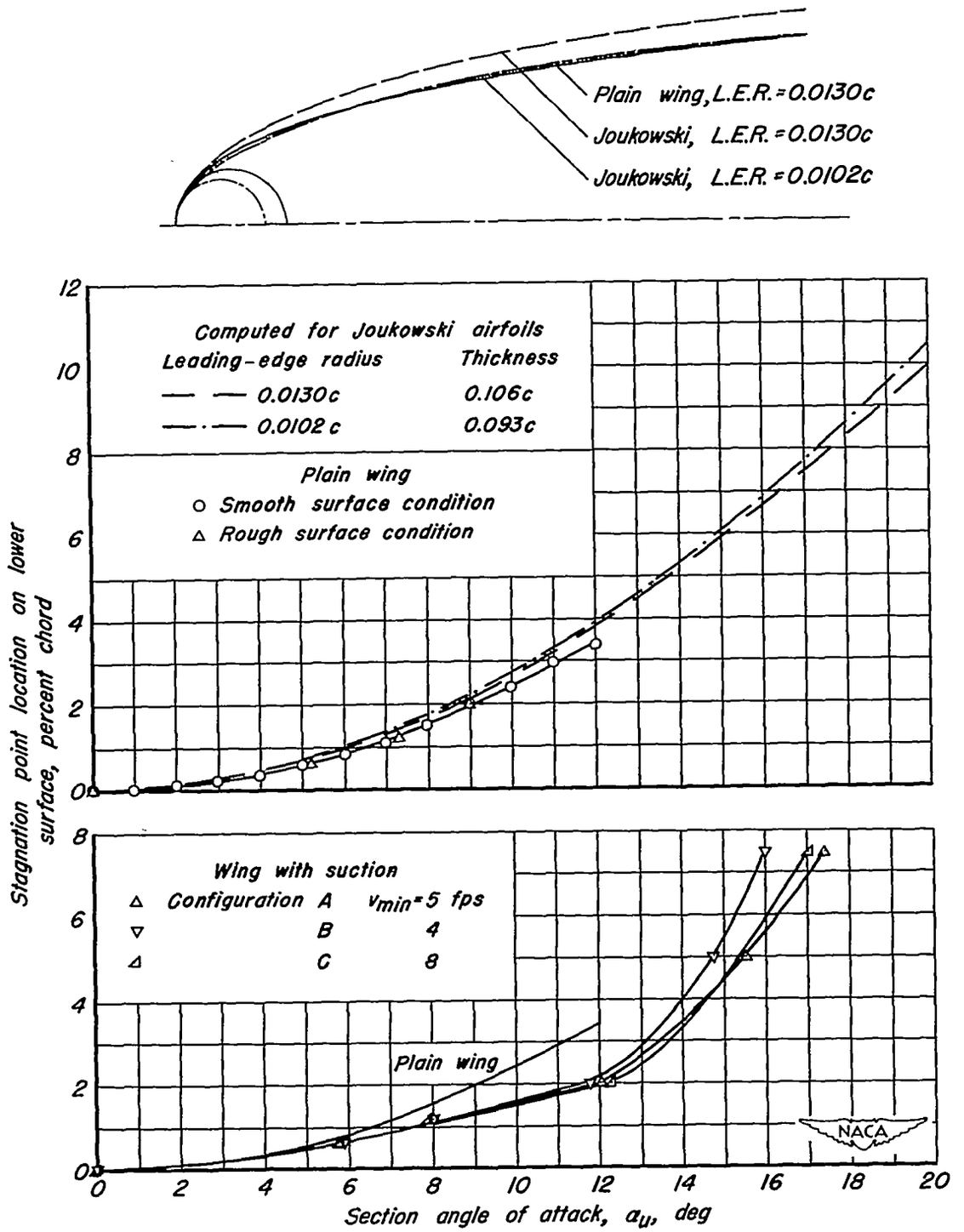

Figure 22.- Variation of stagnation-point location with angle of attack.

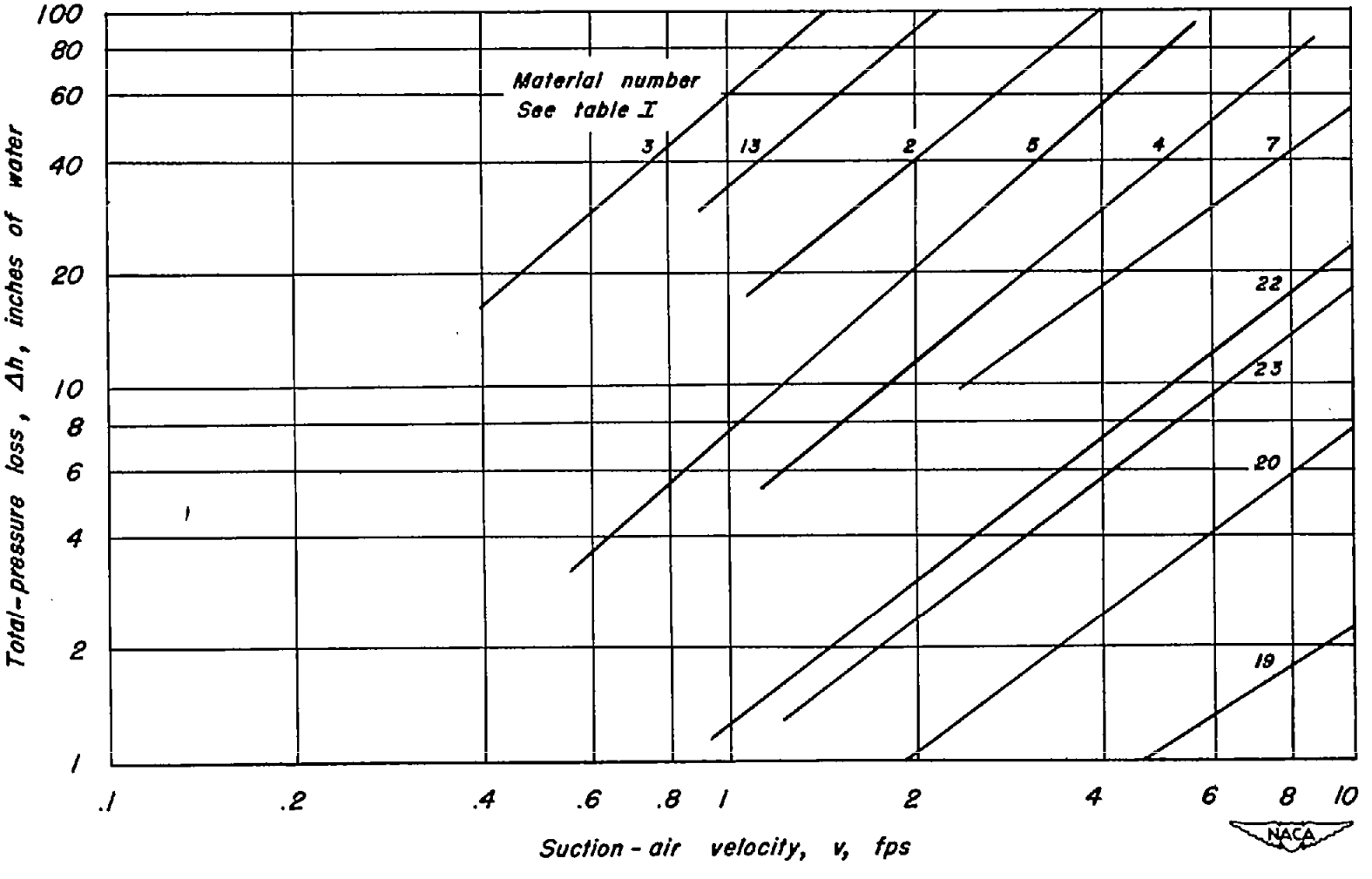

Figure 23.- Flow - resistance characteristics of various porous materials.

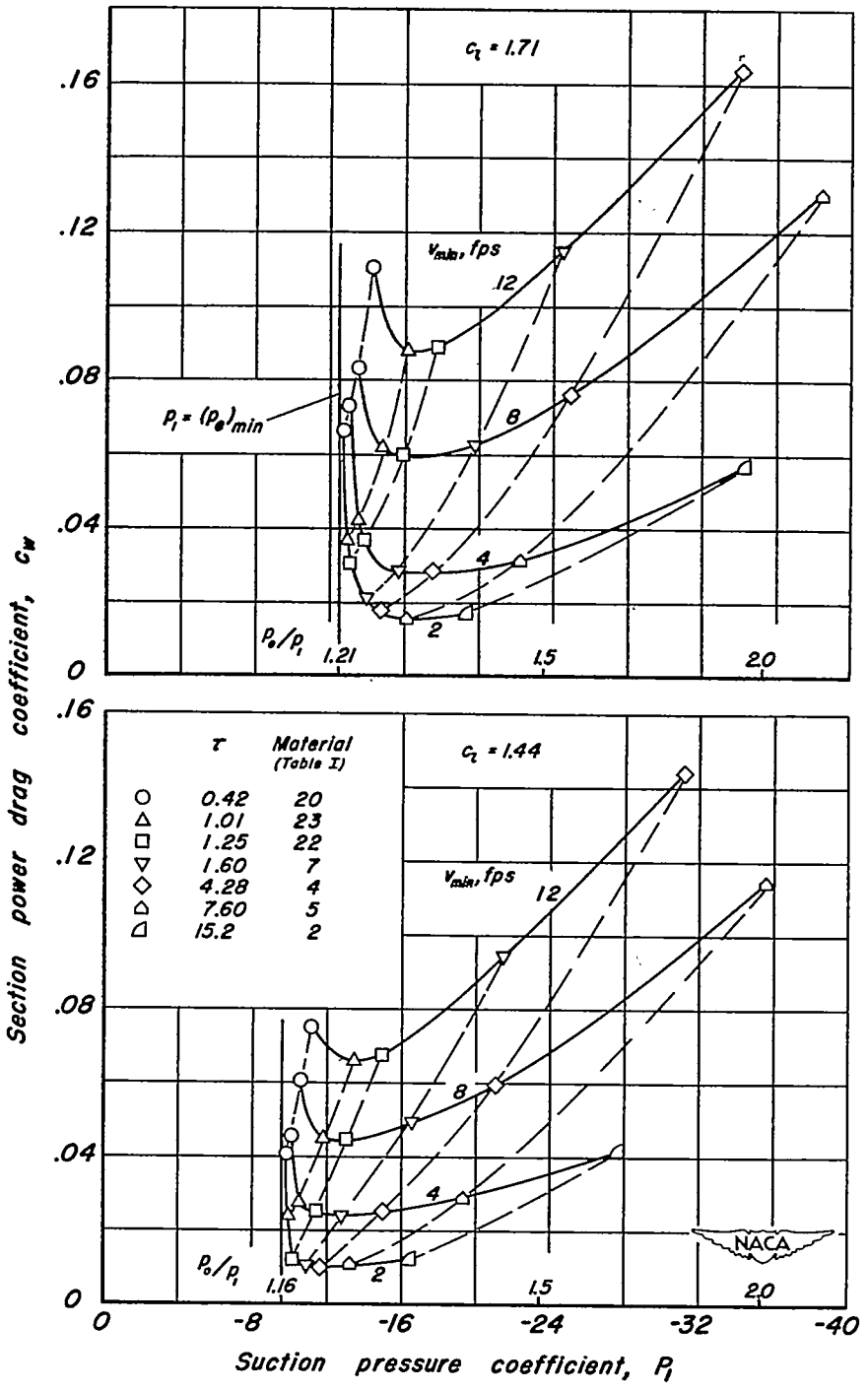

Figure 24.- Calculated section power-drag coefficients for the model with constant thickness of various materials for the porous area from the leading edge to 3-percent chord. q_o = 30 lb/sq ft, p_o = 2116 lb/sq ft.

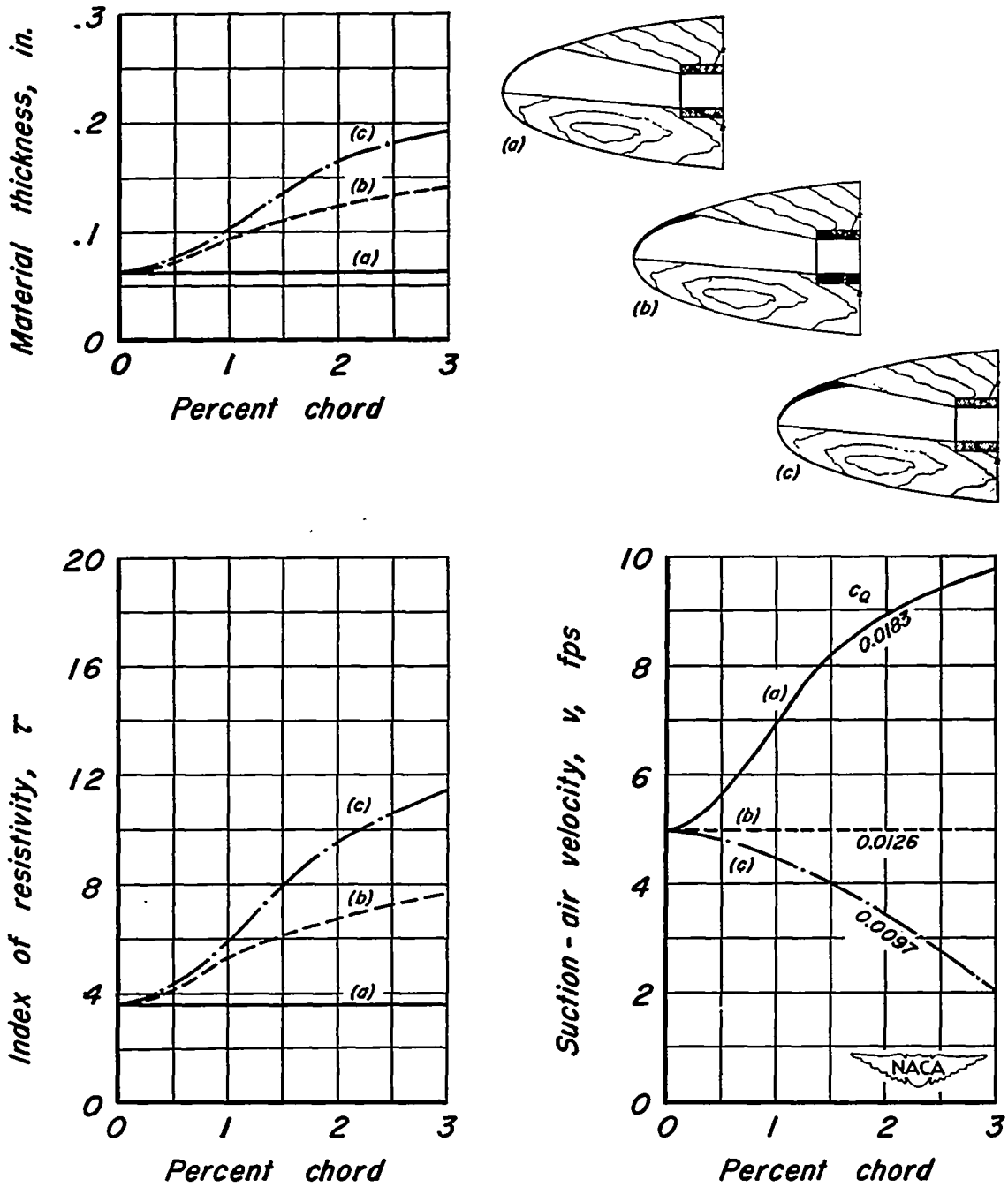

Figure 25.- Calculated suction - air - velocity distributions for various permeability arrangements of material 7 of table I. $c_1 = 1.71$, $q_o = 30$ lb/sq ft, $p_o = 2116$ lb/sq ft.

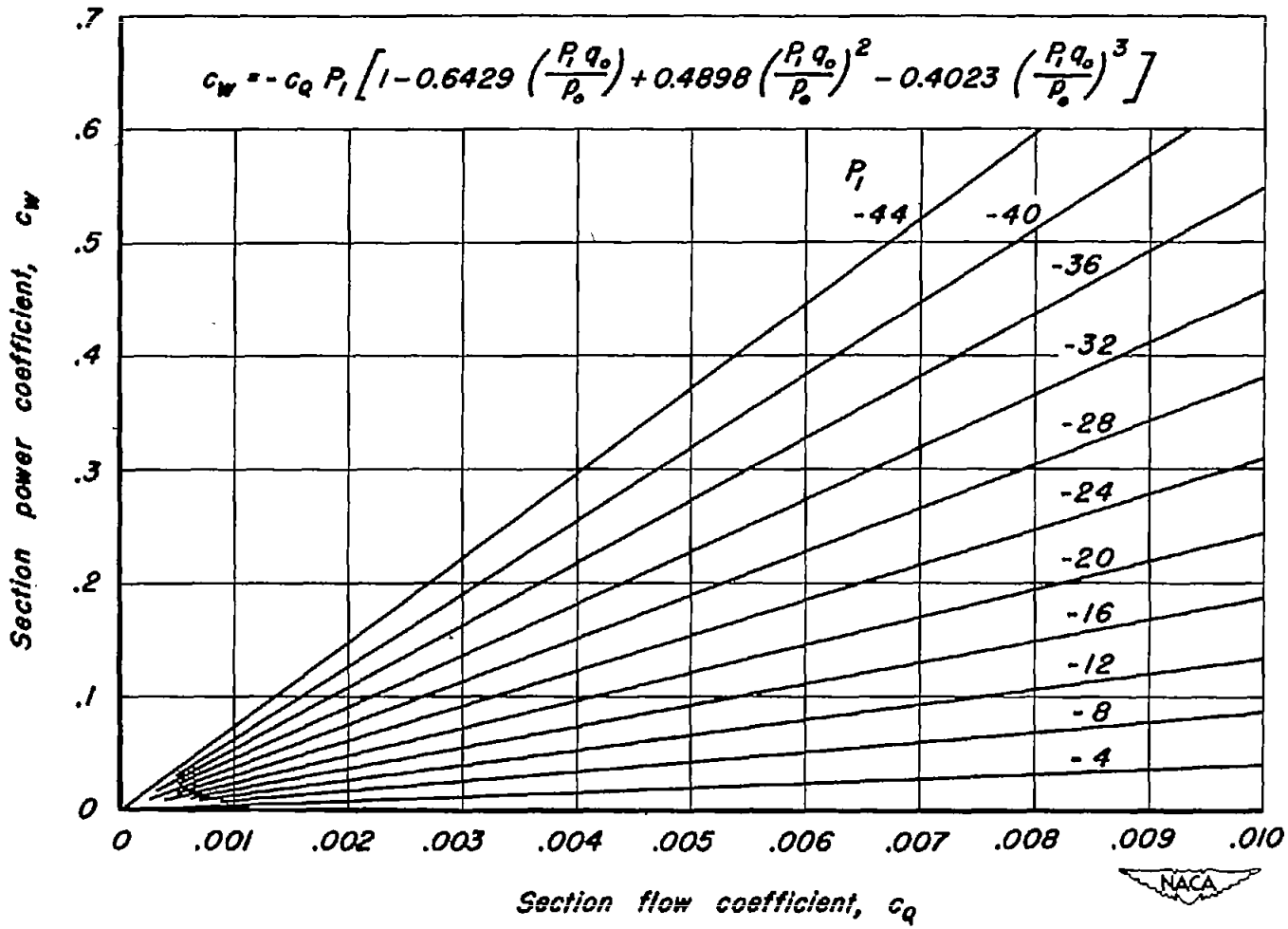

Figure 26.- Variation of section power drag coefficient with section flow coefficient for various suction pressure coefficients. $p_o = 2116$ lb/sq ft, $q_o = 30$ lb/sq ft.

$$c_w = -c_Q P_1 \left[1 - 0.6429 \left(\frac{P_1 q_o}{p_o}\right) + 0.4898 \left(\frac{P_1 q_o}{p_o}\right)^2 - 0.4023 \left(\frac{P_1 q_o}{p_o}\right)^3\right]$$

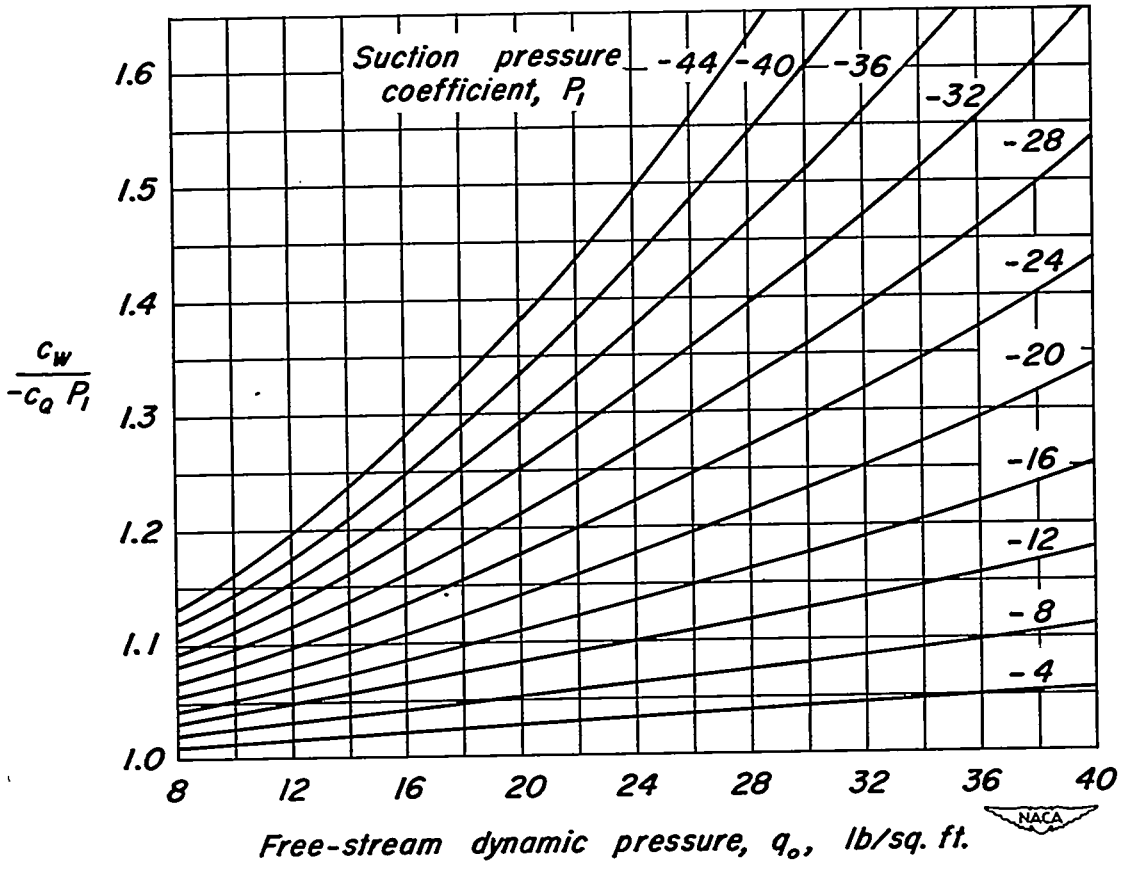

Figure 27.- Variation of the ratio $c_w/-c_Q P_1$ with free-stream dynamic pressure for various suction pressure coefficients. p_o = 2116 lb/sq ft.